Review Vol. 10, No. 12 / December 2023 / Optica 1655

Frequency-bin photonic quantum information

Hsuan-Hao Lu,[1,6] Marco Liscidini,[2] Alexander L. Gaeta,[3] Andrew M. Weiner,[4] and Joseph M. Lukens[1,5,*]

[1]Quantum Information Science Section, Computational Sciences and Engineering Division, Oak Ridge National Laboratory, Oak Ridge, Tennessee 37831, USA
[2]Dipartimento di Fisica, Università di Pavia, Via Agostino Bassi 6, 27100 Pavia, Italy
[3]Department of Applied Physics and Applied Mathematics, Columbia University, New York, New York 10027, USA
[4]School of Electrical and Computer Engineering and Purdue Quantum Science and Engineering Institute, Purdue University, West Lafayette, Indiana 47907, USA
[5]Research Technology Office and Quantum Collaborative, Arizona State University, Tempe, Arizona 85287, USA
[6]luh2@ornl.gov
*joseph.lukens@asu.edu

Received 15 September 2023; revised 22 November 2023; accepted 22 November 2023; published 14 December 2023

Discrete frequency modes, or bins, present a blend of opportunities and challenges for photonic quantum information processing. Frequency-bin-encoded photons are readily generated by integrated quantum light sources, naturally high-dimensional, stable in optical fiber, and massively parallelizable in a single spatial mode. Yet quantum operations on frequency-bin states require coherent and controllable multifrequency interference, making them significantly more challenging to manipulate than more traditional spatial degrees of freedom. In this mini-review, we describe recent developments that have transformed these challenges and propelled frequency bins forward. Focusing on sources, manipulation schemes, and detection approaches, we introduce the basics of frequency-bin encoding, summarize the state of the art, and speculate on the field's next phases. Given the combined progress in integrated photonics, high-fidelity quantum gates, and proof-of-principle demonstrations, frequency-bin quantum information is poised to emerge from the lab and leave its mark on practical quantum information processing—particularly in networking where frequency bins offer unique tools for multiplexing, interconnects, and high-dimensional communications.

https://doi.org/10.1364/OPTICA.506096

1. INTRODUCTION

Electromagnetic modes—i.e., solutions to Maxwell's equations for a specified system—offer a virtually limitless palette for encoding and transmitting data. By populating these modes with photons, information can be carried over global distances and beyond, facilitated in the optical regime of the electromagnetic spectrum by both the ubiquitous fiber-optic infrastructure [1] and a growing toolkit of free-space optical communication technology [2]. Moreover, when the information-carrying photons exhibit nonclassical statistics or correlations, as is the case for fixed-number (Fock) states, squeezed quadrature states, and entangled photon pairs, the modes of interest can carry *quantum* information as well, as required for emerging applications in computing, sensing, and communications. Depending on the physical medium and geometry, a variety of degrees of freedom (DoFs) can be used and potentially combined for defining these modes, including polarization, path, transverse field, orbital angular momentum, time bins, short pulses, and—the focus of this mini-review—frequency bins. Frequency-bin encoding, in particular, can support very large Hilbert spaces, is naturally suited to transmission in single-mode optical fiber, is compatible with integrated photonics, can be readily parallelized and measured via dense wavelength-division multiplexing (DWDM) technology, and is automatically produced by either bulk optical cavities or compact integrated microring-based light sources.

Quantum information processing (QIP) in frequency bins requires three basic capabilities: (i) *production* of quantum states in discrete spectral modes; (ii) *manipulation* of quantum states through quantum operations, or gates; and (iii) *detection* of photons resolved by their spectro-temporal modes. State production and computational-basis detection are inherently strong suits of frequency bins: frequency entanglement appears naturally in continuous-wave (CW)–pumped parametric processes, and frequency-resolved detection is straightforward with DWDM filters and wavelength-selective switches (WSSs). Nonetheless, because frequency-bin quantum gates—and, by implication, projective measurements of multibin superposition states—entail coherent and controllable mixing across multiple spectral modes, state *manipulation* has historically proven a much greater challenge in this DoF than more traditional path or polarization paradigms. Recent years have witnessed remarkable progress in this regard, however, with demonstrations of both nonlinear and electro-optic mixing approaches for control of quantum frequency combs

[3–6], including a complete paradigm for universal quantum information processing known as the quantum frequency processor (QFP): a serial chain of electro-optic phase modulators and Fourier-transform pulse shapers [7]. In light of these advances, frequency-bin encoding is rapidly proving itself a promising framework for quantum information, particularly in networking and communications.

In this mini-review, we summarize the past, present, and future of frequency-bin quantum information processing from both theoretical and experimental perspectives. Our main goal is to provide a comprehensive picture of research in frequency bins by including results from a remarkably broad community working in the same field but with different platforms and with different goals. We believe that such a "specialized" mini-review will favor cross-contamination within this community and, of course, stimulate others to join it. Beginning in Section 2 with a tutorial on the basic features and considerations of frequency-bin quantum processing, we then overview the state of the art in Section 3. Our educated guesses for the future follow in Section 4, in which we envision photonic integration and applications in quantum interconnects as especially exciting developments on the horizon. Throughout our discussion, the triumvirate of production, manipulation, and detection will provide a useful taxonomy for classifying advances and challenges in this field.

To maintain a manageable scope, we concentrate on the intersection of frequency-bin modes (defined by well-separated spectra) and discrete-variable (DV) encoding (qubits or qudits carried by single photons). Related but distinct time–frequency approaches have also received growing attention in recent years, such as discrete frequency bins in the continuous-variable (CV) regime [8–13] and pulsed modes that overlap in both time and frequency [14–22]. For those interested in learning more about these topics, we recommend several excellent reviews [12,16,20–22] for further information. Finally, although frequency-bin encoding can support applications across the QIP spectrum of computing, sensing, and networking, its synergies with classical lightwave communications suggest unique potential in quantum networking specifically. While our outlook in Section 4 accordingly favors communications and networking, omission of other applications should not be construed as a critique of frequency bins in these QIP fields, but rather is a matter of prioritization in this short review.

2. TUTORIAL

A. Sources

In its typical architecture, the frequency-bin DoF consists of a comb of equispaced and nominally identical spectral modes centered at frequencies $\omega_n = \omega_0 + n\Delta\omega$ ($n \in \mathbb{Z}$), to each of which can be added (subtracted) a photon through application of the appropriate creation (annihilation) operator $\hat{a}_n^\dagger$ ($\hat{a}_n$). Although the definition of a "bin" is somewhat flexible and can vary with context, the key feature for our purposes is that each spectral mode is clearly separated from its neighbors, i.e., resolvable with no appreciable overlap. Thus, the state of a pure frequency-bin qudit—d-level carrier of quantum information—can be written as a superposition $|\Psi\rangle = \sum_{j=0}^{d-1} c_j \hat{a}_j^\dagger |\text{vac}\rangle$, where $|\text{vac}\rangle$ denotes the vacuum state over all modes, and $\sum_j |c_j|^2 = 1$. The relative ease of generating frequency entanglement is a key reason for the interest in the frequency-bin DoF. Indeed, spontaneous parametric downconversion (SPDC) or spontaneous four-wave mixing (SFWM) with a CW pump naturally produces broadband frequency-entangled photons [23–26], with exceptionally high efficiency when leveraging copolarized and single-spatial-mode waveguide processes [27–29]. In fact, frequency entanglement is so easily produced that arguably more research has been invested in erasing it than producing it, a feat possible through a judicious combination of pulsed pumping and phase-matching conditions [30–33].

By incorporating spectral filtering either during or after the generation process, the continuous broadband entanglement from CW-pumped SPDC or SFWM can be converted to discrete frequency bins. SPDC followed by an etalon [34–38], SPDC within a cavity [34,39–41], SPDC in a domain-engineered crystal [42], and SFWM in microring resonators (silicon [43–47], Hydex [48–52], SiN [53–57], AlGaAs [58], and AlN [59]) have all been used to generate frequency-bin-entangled states that—compared to their spectrally continuous predecessors—are better matched to low-bandwidth (ns-scale) detection methods leveraging spectral demultiplexing, reach higher brightness (efficiency per unit bandwidth) whenever the nonlinear medium is placed inside the cavity, and can prove significantly more compact with microrings.

Figure 1(a) depicts these approaches for generating frequency-bin-entangled pairs of signal and idler photons of the form $|\Psi\rangle = \sum_{j=k}^{k+d-1} c_j \hat{a}_j^\dagger \hat{a}_{-j}^\dagger |\text{vac}\rangle$, where we have assumed energy conservation based on a pump centered at $2\omega_0$ (ω_0) for SPDC (SFWM). As an example, a two-qubit Bell state $|\Psi^+\rangle \propto |01\rangle_{SI} + |10\rangle_{SI}$ can be prepared by symmetrically selecting four bins from the SPDC/SFWM spectrum, where the basis states $|01\rangle_{SI}$ and $|10\rangle_{SI}$ correspond to two pairs of signal–idler frequency bins—e.g., the jth bin pair and the $(j+1)$th bin pair. It is important to point out that, while spectral entanglement is desirable for frequency-bin QIP, both CW and pulsed configurations still prove useful. The case of a narrowband pump (relative to the bin width) implies the existence of an entanglement substructure, which we show schematically in Fig. 1(a) as lines within each bin (not to be confused with actual resonant behavior) and intra-bin spectral correlations in the top joint spectral intensity (JSI). On the other hand, a broadband pump with properly chosen bandwidth can in principle eliminate these correlations [33,62], leaving a JSI comprising circular islands of spectrally unentangled peaks, i.e., separable in the sense that the intra-bin frequency of one photon is uncorrelated with that of the other [bottom JSI in Fig. 1(a)]. In experiments focused on individual photon pairs where sub-bin structure is unresolvable by the detection process, accounting for the intra-bin entanglement is often unnecessary for describing the results, and can be approximated by the pure bin picture [63–65]. On the other hand, in experiments requiring interference between photons from *independent* pairs, this intra-bin entanglement can significantly degrade purity. In this case, the ultimate goal is to erase spectral entanglement within the defined frequency bins, but retain strong spectral entanglement across multiple bins—a situation possible when the pump bandwidth exceeds that of an individual bin, yet is much smaller than the bin spacing [49–51,66,67].

B. Manipulation

The inherent compatibility of frequency-bin encoding with spectral demultiplexing points to a related, though more general, technique for frequency control: Fourier-transformation pulse

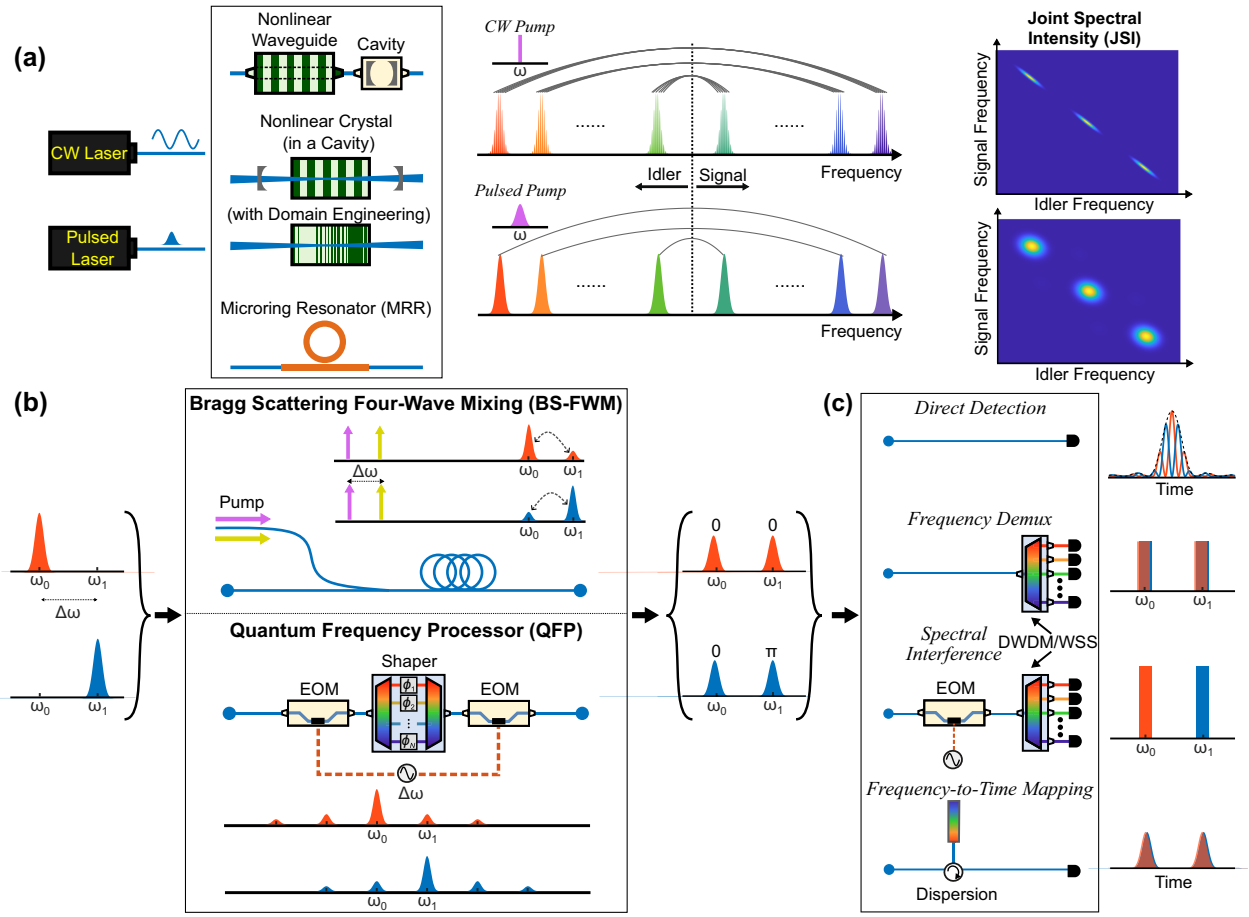

Fig. 1. Basic frequency-bin concepts. (a) *Sources*. Frequency-bin-entangled photons can be produced by a nonlinear medium paired with a resonant structure or engineered phase-matching, excited by either CW or pulsed lasers. (b) *Manipulation*. Parametric nonlinear processes and electro-optic modulation enable controllable spectral operations, as exemplified by frequency-bin beamsplitters based on BS-FWM [60] and the QFP [61], respectively. (c) *Detection*. Available techniques enable measurements in both logical and superposition bases. For (b) and (c), the amplitudes resulting from input states ω_0 (orange) and ω_1 (blue) are traced through by color. [The slight shifts in the orange and blue curves for the second and fourth cases in (c) serve as visual aids only.]

shaping [68,69]. By spatially separating the frequency components of a broadband optical field with, e.g., a grating or prism, focusing them onto a spatial light modulator, and recombining them through a second prism or grating, arbitrary spectral filters can be synthesized, enabling shaping of fs-level features in the optical field. In the quantum domain, pulse shaping of entangled photons was demonstrated first in 2005 [70], followed by further extensions leveraging homebuilt free-space pulse shapers [71–76] and later commercial fiber-pigtailed devices in the telecom C-band (1530–1570 nm) [77–81]. From the perspective of frequency-bin encoding specifically, the fact that the input spectrum of interest contains bins that are clearly separated from their neighbors implies that line-by-line pulse shaping can be invoked—a classical technique in which each line of a frequency comb is individually addressable, allowing for completely arbitrary fields that fill the entire temporal period [82,83]. Thus, fully arbitrary filters (amplitude and phase) are available to frequency-bin-encoded states, as long as the spacing $\Delta\omega$ comfortably exceeds the resolution of the pulse shaper utilized.

Nevertheless, such filters are not by themselves sufficient for QIP, where one needs to be able to interfere frequency bins as well. In principle, such interference can be realized through ultrafast time gating. Indeed, in many of the early quantum pulse shaping experiments, biphoton sum-frequency generation (SFG) without an ancilla pump field was used to enable observation of sub-ps features in the two-photon state [70,72,74–81]. But SFG suffers from extremely low quantum efficiencies ($\sim 10^{-5}$ at best without a pump [78]), making it impractical for QIP applications. Alternatively, with sufficiently fast direct detection, one could postselect on interference between multiple bins [84]. Yet this approach is challenging with current detector jitters and thus has not been implemented experimentally for typical bin spacings of tens of GHz and beyond. Instead, experimental demonstrations so far have focused on controllable spectral interference through either nonlinear- or electro-optic approaches that provide the operation of interest without temporal postselection.

Various nonlinear optical processes can produce frequency coupling, interference, and conversion between different spectral components, where classical pump fields enable near-unity efficiencies in contrast to processes like biphoton SFG above. However, for quantum applications, there are only a few $\chi^{(2)}$ and $\chi^{(3)}$ processes that yield a unitary relationship between two frequency components that do not add noise and are analogous to a *beamsplitter* transformation. These processes are known as quantum frequency conversion (QFC). For the case of a $\chi^{(2)}$

interaction, the process of sum-frequency conversion or parametric downconversion with one of the low-frequency components serving as a pump field results in the following unitary relation between the input and output amplitudes of the two other fields (here two generic frequency bins j and k):

$$\begin{pmatrix} \hat{a}_j^{\text{out}} \\ \hat{a}_k^{\text{out}} \end{pmatrix} = \begin{pmatrix} \cos\theta_{NL} & e^{i\phi}\sin\theta_{NL} \\ -e^{-i\phi}\sin\theta_{NL} & \cos\theta_{NL} \end{pmatrix} \begin{pmatrix} \hat{a}_j^{\text{in}} \\ \hat{a}_k^{\text{in}} \end{pmatrix}, \quad (1)$$

where $\hat{a}_{j,k}^{\text{in}}$ and $\hat{a}_{j,k}^{\text{out}}$ are the input and output annihilation operators, with the higher-frequency bin historically denoted as the "signal" and the lower-frequency bin the "idler"; θ_{NL} is the nonlinear parameter that depends on the pump amplitude, the length of the interaction, and the nonlinear susceptibility; and ϕ is the relative phase among the three fields. Similarly, for $\chi^{(3)}$ interactions, the process of Bragg-scattering four-wave mixing (BS-FWM) with two strong pump fields leads to an identical relation [Eq. (1)] where the nonlinear parameter depends on $\chi^{(3)}$ and the product of the two pump-field amplitudes [85].

A key advantage of using such nonlinear optical interactions is that the frequency separation between the fields can be tuned from a few GHz to >10 THz and even span the visible to mid-infrared regimes. Such QFC can be valuable not only for converting single photons and quantum states of light back and forth between quantum memories in atoms and diamond color centers (from nitrogen and silicon vacancies) in the near infrared to the telecommunications bands in optical fibers where the losses are low, but also for performing quantum logic operations on frequency qubits [60].

QFC based on nonlinear interactions was first described by Kumar [86] using a $\chi^{(2)}$ process and observed in bulk potassium titanyl phosphate (KTP) [87]. This was extended to periodically poled lithium niobate (PPLN) waveguides [15,17,88–92] with internal conversion efficiencies as high as 90% [88]. More recently, high QFC efficiencies have been demonstrated in tightly confining PPLN waveguides to realize chip-based single-photon detection [93]. Such $\chi^{(2)}$ systems have also been used to facilitate long-distance entanglement transfer [94–98] and connect quantum memories via optical fibers [99–103]. For the case of $\chi^{(3)}$ interactions, BS-FWM does not require the use of a medium with inversion symmetry and thus can be realized in various photonic platforms consisting of amorphous materials including optical fibers [104], as first demonstrated by McGuiness *et al.* [105], and in chip-based waveguides. Experiments using optical fiber at liquid nitrogen temperatures to avoid Raman noise have demonstrated internal QFC efficiencies as high as 99% [60,106]. Experiments in SiN chip-based devices [107–109] have demonstrated QFC efficiencies as high as 60%. Additional experiments in SiN microresonators showed QFC of a quantum dot that was fiber-coupled to the chip [109].

While most experiments on QFC—including recent efforts in novel media such as hydrogen-filled hollow-core fibers [110]—have focused on demonstrating high efficiencies for spectral translation, studies [60] did explore the concept of using QFC to realize a frequency qubit for quantum logic operations whose state could be generated and manipulated through QFC processes. Further work showed that by using multiple pump waves to extend coupling between multiple signals and idlers, it was possible to realize a bosonic N-level system [111] and frequency-domain boson sampling [112].

Electro-optic phase modulators (EOMs) provide another avenue for controllable spectral interference. A longstanding component in lightwave communications [113], EOMs rely on the electro-optic effect of materials such as lithium niobate to modulate the phase of an optical field according to an applied radio-frequency (RF) voltage. As linear devices (from the perspective of the optical domain) EOMs transform single-photon states with the same efficiency as bright classical states; after the first theory and experiments on single [114,115] and entangled photons [116–119] were reported in 2008–2010, follow-up experiments have expanded to manipulation and measurement techniques such as temporal gating [120], time lensing [121,122], and spectral shearing [123].

In the case of frequency bins, an EOM driven by a waveform periodic at the mode spacing $\Delta\omega$ can be viewed as a spectral interferometer, with mixing coefficients determined through the Fourier expansion [116,124,125]. By themselves, the presence of both upper and lower sidebands prevents EOMs from implementing arbitrary unitary operations in a finite-dimensional Hilbert space, even in theory [61]. Although unwanted sidebands can be removed at the expense of flux, either through direct spectral filtering [126] or Mach–Zehnder interference as in single-sideband modulation [127], joining EOMs with pulse shapers in series allows residual sidebands to be returned to the subspace of interest through sequential interference, enabling the scalable synthesis of truly arbitrary frequency-bin unitaries with in principle 100% efficiency [7]. Dubbed the "quantum frequency processor" (QFP) [63], this approach has been leveraged in a variety of experimental demonstrations, as discussed further in Section 3.B below.

To elucidate the distinct principles through which nonlinear- and electro-optic methods approach frequency gate synthesis, Fig. 1(b) depicts the spectra resulting from an input at ω_0 (ω_1) in orange (blue) for the 50/50 frequency beamsplitter, or Hadamard gate. Mathematically, such an operation can be expressed by a 2×2 transformation matrix:

$$U_{2\times 2} = \frac{1}{\sqrt{2}} \begin{pmatrix} 1 & 1 \\ 1 & -1 \end{pmatrix}, \quad (2)$$

mapping the basis states, $|0\rangle$ (ω_0) and $|1\rangle$ (ω_1), to two equal superposition states. We have chosen the standard definition of H, which deviates from Eq. (1) with $(\theta_{NL}, \phi) = (\pi/4, \pi)$ only in terms of a trivial phase convention; regardless, the phase between the output frequencies from a such a beamsplitter differs by π depending on the input (either ω_0 or ω_1). Yet while both paradigms lead to the same outputs, they do so in markedly different ways. BS-FWM relies on the continuous transfer of energy from one bin to the other, the amount of which is controlled by θ_{NL}. On the other hand, the QFP initially spreads input photon probability amplitudes into adjacent sidebands with the first EOM (spectra shown); then by applying appropriate line-by-line phases on the pulse shaper and traversing the second EOM, the desired two-mode output is obtained.

C. Detection

Once a frequency-bin quantum state is generated and manipulated as desired, some form of quantum measurement is required to either validate the operation (e.g., via tomography) or complete a desired QIP protocol. Figure 1(c) displays several of the main approaches available for frequency-bin measurement, depicting their responses to the superposition states in Fig. 1(b) as a concrete way to distinguish their strengths and weaknesses. For sufficiently

small $\Delta\omega$ (relative to detector jitter), one can directly measure the interference fringes in the single- or two-photon wavepacket [40,128–130]; this can distinguish between the two superposition cases in Fig. 1(c) through time shifts in the interference fringes. However, if the bin-spacing is large, these fringes are washed out and any phase-dependent differences vanish. When $\Delta\omega$ aligns with multi-GHz spacings common on the DWDM grid, one straightforward measurement procedure simply demultiplexes the different bins to unique detectors. While valuable for computational-basis measurements, phase differences again prove undetectable.

Discriminating between superposition states with slow detectors is possible, however, by preceding the demultiplexer with controllable interference [using either the nonlinear or electro-optic techniques displayed in Fig. 1(b)]. We show a possibility using the EOM tuned to interfere ω_0 and ω_1 with equal weights. In this case, the two superposition states do present unambiguous detection signatures: the equal-phase case (orange) emerges as ω_0 while the π-phase-shifted case (blue) as ω_1. The EOM's ability to facilitate projective superposition measurements has enabled full quantum state tomography of a variety of frequency-bin entangled states, either with multi-EOM QFPs [63,131] or single EOMs followed by filters or demultiplexers [46,47,50,55,57,132]. One final measurement approach of note leverages frequency-to-time (FTT) mapping using dispersion (long fibers or chirped fiber Bragg gratings) [32,133,134]. This technique provides the same information as frequency demultiplexing—i.e., spectral amplitude, but not phase—yet offers the practical advantage of requiring only one detector for all bins per photon.

As an aside, spatial Hong–Ou–Mandel (HOM) interferometry [135]—as distinguished from spectral HOM in Section 3.B—has also been shown to be sensitive to the spectral phase of two frequency-bin qubits, making it useful for entanglement verification [136–141]. (Incidentally, to our knowledge, Ref. [138] was the first paper to coin the term "frequency bin.") Yet because this spatial HOM method requires the two photons to occupy the same pair of bins and does not extend to qudits [142], it is somewhat less general than the four methods we have focused on here, for which the key takeaway is: while spectral *amplitude* measurements are straightforward (with either demultiplexing or FTT mapping), *phase* measurements require either fast detectors or spectral interference.

3. STATE OF THE ART

A. Sources

In the current landscape, the generation of frequency bins hinges primarily on SPDC and SFWM. The former approach, based on SPDC, is commonplace in bulk quantum systems and predominantly uses PPLN [119,132,139,143–145] or periodically poled potassium titanyl phosphate (PPKTP) [11,42,146], offering extensive versatility in terms of applications and wavelength ranges. Owing to the high efficiency of second-order nonlinear interactions, the generation efficiency in SPDC-based systems is typically on the order of 10 kHz/mW. This efficiency leads to coincidence counts from a few Hz/mW to 100 Hz/mW depending on the photon collection efficiency and the specific experimental apparatus. As usual with parametric sources, a compromise must be struck between count rate and the coincidence-to-accidental ratio also in the generation of frequency bins.

When using SPDC, frequency bins are usually generated using Fabry–Pérot cavities, in which the free spectral range (FSR) has varied from some 500 MHz [143] to 25 GHz [63] in experimental examples, depending on the cavity geometry. These are the systems in which the largest Hilbert spaces with frequency bins have been demonstrated, with generation in up to 60 different modes [11]. Although the majority of implementations are focused on the telecom C-band, periodic poling can be engineered to operate at very different wavelengths, including the telecom O-band (1260–1360 nm) [145]. In addition, the signal and idler beams can be designed to operate in the telecom and visible ranges, respectively [143]. Finally, in bulk systems, the resonance linewidth can easily reach a few MHz, facilitating interface with atomic memories [143]. These versatile characteristics of SPDC-based systems make them an invaluable tool in the burgeoning field of quantum information science.

In contrast, SFWM-based approaches are primarily implemented in integrated platforms, which can provide the temporal and spatial confinement required to enhance SFWM and ensure sufficient generation efficiency. SFWM is also particularly appealing for integrated platforms owing to its compatibility with complementary metal–oxide–semiconductor (CMOS) devices. Frequency bins have been generated in Hydex [48–52], SiN [54,55,57,147], and silicon [46,47,148] ring resonators, exhibiting pair generation typically of around 1 MHz/(mW)^2 or higher.

In integrated devices, frequency-bin spacings can vary from a few GHz to a few THz. However, the detection techniques (as discussed in Section 2.C) have currently limited the bin spacing of a fully characterized on-chip system to 200 GHz due to the available electro-optic bandwidth [50]. When photons are generated in a single ring resonator, there is a trade-off between the bin separation and the resonator's FSR; smaller FSRs are associated with lower generation rates [149]. However, by employing multiple ring resonators one can control the bin spacing on-demand using thermal shifters [47]. In this case, the minimum frequency-bin distance is only limited by the resonance linewidth, that is, by the quality factor of the resonator. Today, there have been demonstrations of entanglement in up to eight pairs of frequency-bin modes [57] for integrated devices. The compatibility with CMOS technology and the ability to generate and control frequency bins in the telecom wavelength range with high efficiency make SFWM a significant player in QIP. In the majority of experiments reported to date, sources utilizing either SPDC or SFWM methodologies have been pumped using a CW laser. This is because long interaction lengths (as in PPLN waveguides) or resonant field enhancements (as in ring resonators) guarantee a sufficient generation rate. However, these sources can also operate using pump pulses [49–51,67], an approach that has a specific utility. The use of pump pulses is essential to eliminate quantum correlations within each frequency bin, a requirement crucial for exploiting the interference of multiple pairs.

The generation of frequency bins through SPDC or SFWM naturally results in entanglement with negative spectral correlations [cf. Fig. 1(a)], which originates from the principles of energy conservation, phase-matching conditions, and the presence of resonant field enhancement. Yet, in the last few years, there has been substantial progress in designing sources capable of directly generating specific entangled states, circumventing the need for subsequent manipulation of the produced state. This has been

achieved by modifying the spatio-spectral properties of the pump [47,132,150], tailoring the phase-matching function through domain engineering [42], or fabricating a source with multiple nonlinear elements. In the last approach, the state is constructed "piece-by-piece," leveraging the coherent superposition of either SPDC [139] or SFWM [46]. This approach is particularly effective in integrated devices, in which reconfigurability is a sought-after attribute. By employing tuning elements, such as micro-heaters, precise control and on-demand reconfiguration can be achieved [46].

In Table 1 we summarize all the previous considerations and the state of the art in terms of material platforms, wavelength of operation, frequency spacing, and generation bandwidth. The examples shown are not intended to be exhaustive, but rather representative of the variety in this field, from which it is clear that frequency bins are a flexible and valuable DoF to encode quantum information in a plethora of systems.

B. Manipulation

Introduced in Section 2.B, the frequency beamsplitter can be viewed as the quintessential frequency-bin gate in terms of its importance and influence in establishing and advancing the state of the art in this field. A successful frequency-bin Hadamard overcomes the fundamental challenge of frequency-bin manipulation: while applying phase shifts is easy (just use a pulse shaper), controllable interference is not, especially when compared to alternative DoFs such as path or polarization where beamsplitters and waveplates are readily available. Consequently, the beamsplitter functions as perhaps the simplest nontrivial frequency-bin operation.

Moreover, the frequency beamsplitter enables demonstration of *frequency-domain* HOM interference [152], as depicted in Fig. 2(a): when two photons enter the device, one at ω_0 and the other at ω_1, quantum interference causes the photons to bunch,

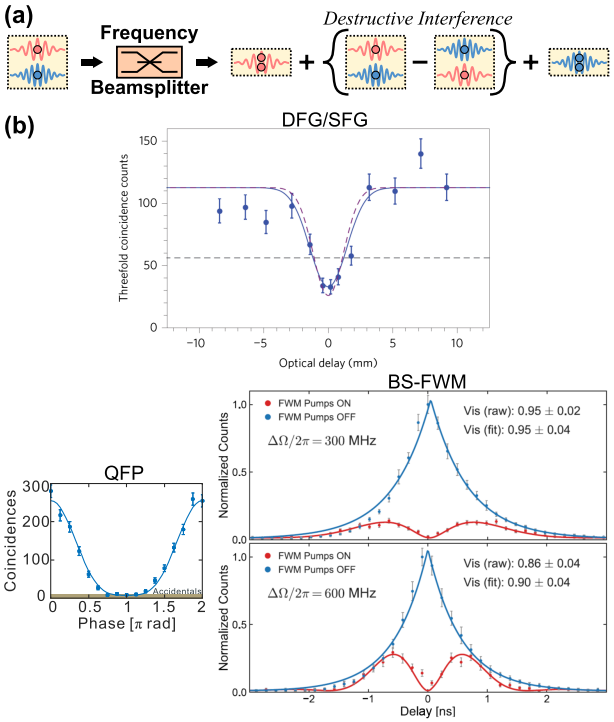

Fig. 2. Frequency-bin HOM. (a) Through quantum interference, single photons entering a frequency beamsplitter in distinct bins can coalesce, suppressing cross-spectral coincidences at the output. (b) Beamsplitters based on $\chi^{(2)}$ (DFG/SFG) [153], electro-optic (QFP) [63], and $\chi^{(3)}$ (BS-FWM) processes [56] have all observed this behavior. Images reproduced with permission from Springer Nature [153] and the American Physical Society [56].

i.e., emerge as a superposition of both at ω_0 and both at ω_1. The probability to measure them at different frequencies is ideally zero, the degree of which can be quantified through the visibility $\mathcal{V}$,

Table 1. Frequency-Bin Sources[a]

Refs.	Platform	Wavelength(s)	Bin Spacing	Bandwidth (# Probed Modes)	Pump
[144]	PPLN/WG/PS	C-band	22 GHz	∼40 nm (16)	CW at 773 nm
[63]	PPLN/WG/FP	C-band	25 GHz	>20 nm (50)	CW at 774 nm
[145]	PPLN/WR	C-band	12.5 GHz	>100 nm (16)	CW at 780 nm
[143]	PPLN/FP	1436 nm/606 nm	423 MHz	N/A (2)	CW at 426 nm
[146]	PPKTP/WG/FP	O-band	5 GHz	∼1.4 nm (19)	CW at 658 nm
[42]	8b-KTP/DE	C-band	500 GHz	>30 nm (8)	1.2 ps at 778 nm
[150]	AlGaAs/WG/FP	C-band	∼30 GHz	∼1 nm	6 ps at 773 nm
[50]	Hydex/MRR	C-band	200 GHz	>40 nm (10)	570 ps at 1550 nm
[52]	Hydex/MRR	C-band	50 GHz	∼23.6 nm (59)	CW at 1550 nm
[54]	SiN/MRR	C-band	385 GHz	∼50 nm (6)	CW at 1551 nm
[55]	SiN/MRR	C-band	49.6 GHz	∼32 nm (38)	CW at 1551 nm
[151]	SiN/MRR	C-band	97.8 GHz	∼35 nm (6)	CW at 1550 nm
[57]	SiN/MRR	C-band	40.5 GHz	>33 nm (49)	CW at 1551 nm
[147]	SiN/MRR	C-band	199 GHz	>7.5 nm (3)	CW at 1550 nm (integrated)
[46]	Silicon/MRRs	C-band	19–57 GHz	∼40 nm (2)	CW at 1550 nm
[47]	Silicon/MRRs	C-band	15 GHz	∼40 nm (4)	CW at 1550 nm

[a]Summary of the state of the art of the sources for the most popular material platforms. The platform column indicates the material and the filtering geometry (DE, domain engineering; FP, Fabry–Pérot; MRR, microring resonator; PS, pulse shaper; WG, waveguide; WR, waveguide resonator). We report the generation bandwidth (when available) and the number of modes that have been investigated, but omit brightness due to the difficulty in standardizing results across the reference list in a meaningful way.

obtained by comparing the coincidence rate at maximal overlap to the case when quantum interference is eliminated (either due to temporal mismatch or detuning the beamsplitter). Figure 2(b) shows three experimental results: a $\chi^{(2)}$ beamsplitter relying on difference- and sum-frequency generation (DFG/SFG), attaining $\mathcal{V} \approx 0.71$ [153]; a QFP beamsplitter, reaching $\mathcal{V} \approx 0.97$ [63]; and a BS-FWM beamsplitter, demonstrating $\mathcal{V} \approx 0.95$ [56]. (A probabilistic electro-optic version has also been realized, for which $\mathcal{V} \approx 0.84$ was observed after accidental subtraction [126].) Interestingly, the deviation from $\mathcal{V} \approx 1$ in many of these experiments has been attributed to multiphoton noise and not the beamsplitter operation, indicating that these results are limited primarily by the input state rather than the frequency-bin gate itself. Frequency-bin quantum process tomography, as recently pioneered on the QFP beamsplitter [6], offers a valuable future direction to further clarify and isolate sources of noise in all of these instantiations.

These HOM results not only confirm successful beamsplitter operation, but they do so via an authentic nonclassical effect that thus substantiates the quantum compatibility of the gate. Nevertheless, spectral HOM interference only scratches the surface of possibilities for frequency-bin state manipulation. For example, two frequency beamsplitters separated by a phase shift can be used to produce a Mach–Zehnder interferometer [154], the basic idea behind Ramsey interference of single frequency-bin qubits [60]. Similarly, a frequency beamsplitter applied to the pump photons *before* SPDC/SFWM can be leveraged to produce two-photon energy correlations not possible with a single-line pump, i.e., exciting the pair-production process with multiple coherent pump lines (whether generated by a frequency beamsplitter or extracted from a frequency comb) can produce entangled photons whose frequencies are *positively* correlated—rather than negatively correlated as demanded in CW pumping [Fig. 1(a)]. These ideas recently enabled production of all four frequency-bin Bell states in a fixed set of four frequency bins as shown in Fig. 3(a) [132]. Extending beyond beamsplitters, the QFP paradigm has led to the demonstration of a coincidence-basis controlled-NOT gate [64], which—along with the single-qubit Hadamard and phase gates—formally defines a universal gate set for linear-optical computing in frequency bins [7,157]. And with both arbitrary single-qubit unitaries [155] and parallel two-photon gates realized to date [63] [Fig. 3(b)], the QFP appears well positioned for reconfigurable and parallelizable state control in quantum communications.

The realization of parallel gates spanning many frequency bins [61,63,158] points to the wider opportunity for manipulating high-dimensional qudits as well. High dimensionality represents one of the inherent advantages of frequency-bin encoding, although it is important to recognize that qudits do not circumvent the fundamental challenges associated with scaling QIP systems. The Hilbert space dimension D for n d-level qudits is $D = d^n$; thus, increasing d leads only to a polynomial increase in dimensionality, compared to the exponential scaling associated with n—it is this latter behavior that underpins the exceptional scaling of quantum computation. Notwithstanding, the extra information carried per photon in the qudit context does provide practical advantages in quantum communications, such as improved robustness to noise [159,160] and stronger Bell-inequality violations [161]. The first experimentally realized high-dimensional frequency-bin gate was the tritter—the 3×3 extension of the beamsplitter—synthesized on a QFP driven by a dual-tone RF signal (sinewaves at $\Delta\omega$ and $2\Delta\omega$) [61]. By leveraging the expanded set of tools available for time-bin manipulation (e.g., delay interferometers), frequency–time hyperentanglement has opened up additional opportunities for high-dimensional state control, including deterministic controlled-unitaries that have been used for generating ultrahigh-dimensional Greenberger–Horne–Zeilinger states [144] and d-level cluster states [5,162].

C. Detection

A promising trend in frequency-bin state detection has appeared in recent years, which attempts to exploit nonstandard features of frequency-bin interference—aspects that have previously been viewed as roadblocks for implementing quantum measurements—and build custom characterization methods that leverage them directly. For example, while RF arbitrary waveform generation

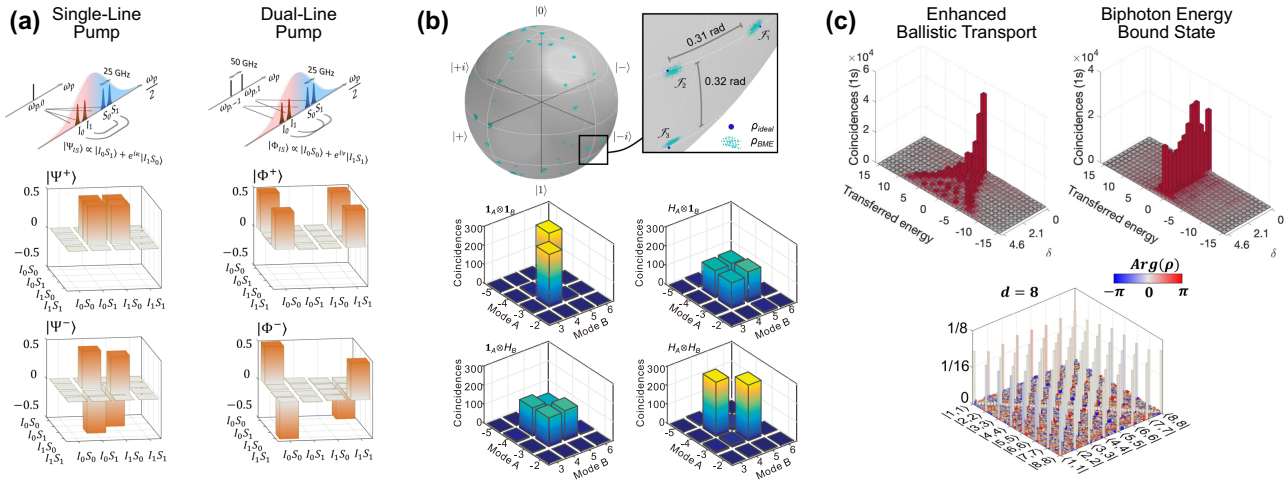

Fig. 3. Manipulation and measurement of frequency-bin qubits and qudits. (a) Bell basis synthesizer (real parts of each density matrix shown) [132]. (b) Arbitrary single-qubit (top) [155] and parallel qubit (bottom) [63] operations. (c) Measurements using sinewave electro-optic modulation can be viewed as a quantum walk (top) [156] that can be leveraged for high-fidelity inference of high-dimensional states (bottom) [57]. Images reproduced with permission from the American Physical Society [132,155] and a Creative Commons Attribution 4.0 International License (https://creativecommons.org/licenses/by/4.0/) [57,156].

with up to ∼25 symbols per period at $\Delta\omega/2\pi \gtrsim 10$ GHz is possible with state-of-the-art direct digital synthesizers [163], it is significantly more expensive and challenging to implement than low-noise sinewave modulation. By the Jacobi–Anger expansion, single-frequency phase modulation with amplitude δ corresponds to the Fourier series $e^{i\delta \sin \Delta\omega t} = \sum_{n=-\infty}^{\infty} J_n(\delta) e^{in\Delta\omega t}$; for frequency-bin measurement, sinewave modulation therefore interferes bins separated by $n\Delta\omega$ according to the Bessel function weight $J_n(\delta)$. For high-dimensional measurement in particular, the nonuniform oscillatory behavior and infinite support (in n) of these Bessel functions deviate strongly from uniform d-dimensional mixing desired for measurements in, e.g., bases mutually unbiased with respect to the computational basis [164,165].

The QFP addresses this challenge through a cascade of EOMs and pulse shapers, which has enabled realization of a variety of frequency-bin gates with high fidelity and success probability—all with sinewave modulation so far (single- or dual-tone) [6]. Alternatively, in the simpler application of projective measurements (as distinct from $d \times d$ gates), preceding the EOM in Fig. 1(c) with a pulse shaper can precompensate for unequal mixing weights through Procrustean amplitude filtering [50,55]. Both approaches tackle the "Bessel function problem" through additional components that increase complexity and add loss—loss that in the Procrustean version is not only technical, but intrinsic. Yet recent work has discovered that leveraging the unequal Bessel function weights as-is still provides valuable information into the frequency-bin quantum state. Recognizing that tuning the modulation index δ produces a quantum walk in the frequency domain [156,166], markedly different energy correlations have been observed by initially in-phase frequency-bin-entangled photons (enhanced ballistic transport) compared to those with alternating π phase shifts (biphoton energy bound state), as shown in Fig. 3(c) [156].

The hypothesis that similar phase-dependent behavior could be sufficient to work backward and *infer* properties of the state has recently been leveraged for both entanglement certification [167] and complete tomography [57] of frequency-bin states. In the latter case, spectrally resolved coincidences obtained from randomly chosen modulation indices δ combined with Bayesian inference techniques enabled full density matrix reconstruction of the output from a SiN microring, consisting of entangled qudits up to $d = 8$ bins each—a 64-dimensional Hilbert space [Fig. 3(c)]. Such spectral interference phenomena can be used for characterizing features of quantum channels as well, as shown experimentally for dispersion measurements [168] and nonlocal delay sensing [169]. Incidentally, these latter two examples exploited relatively wide frequency bins generated by SDPC followed by spectral filtering with a pulse shaper, for which the ratio of bin spacing to bin width (finesse) was only ∼2−3, highlighting the general applicability of these interference techniques to platforms that deviate strongly from the high-finesse cavities typically associated with frequency-bin encoding. Add to these examples the use of RF-detuned Vernier modulation to temporally magnify interference otherwise lost in detector jitter [67], and frequency-bin characterization efforts continue to show an ability to expand and thrive within the confines set by the Jacobi–Anger expansion.

4. FUTURE SPECULATION

A. On-Chip Integration

Thus far, we have seen significant advances in tools that can manipulate frequency-bin-encoded photons with remarkable precision. These seminal experiments have validated many of the essential functionalities for general QIP tasks. However, the current state of these experiments is limited to small-scale systems with a restricted number of dimensions and particles, highlighting the need for further research to scale up these approaches. For instance, there exists a substantial gap between the seemingly unbounded dimension of frequency-bin entanglement in photon sources and the dimensionality that can be fully controlled. Although it has been shown theoretically that QFP operations can be extended to higher dimensions by adding extra RF harmonics to the EOM drives [61,131], in practice the bandwidth of the EOMs and the spectral resolution of the pulse shaper that defines the minimum bin spacing set limits on the complexity of these operations. On the other hand, deepening a QFP circuit serially by introducing extra EOMs and shapers can address larger Hilbert spaces for a fixed RF bandwidth [7]. However, this will inevitably introduce a significant amount of optical loss, which presents an even greater challenge, particularly in the realization of N-photon quantum gates whose success probability scales like η^N, with η the total system efficiency. Therefore, utilizing photonic integrated circuits either to minimize optical loss or to realize photon sources that are more compatible with existing RF capabilities (i.e., with reduced bin spacing), will be crucial for realizing the full potential of the frequency DoF. Inspired by the path-encoded teleportation framework used to organize a recent review of hybrid quantum photonics [170], we kick off our discussion of future speculation by envisioning a chip-based quantum teleporter for frequency-bin qubits (Fig. 4). We will break down each chip into its various building blocks and examine how some of the latest developments in the field could potentially fulfill each of these functions.

As a fundamental protocol for long-distance quantum communication, quantum teleportation is expected to play a pivotal role in scalable quantum networks. In the ideal scenario, Alice and Bob preshare a pair of entangled photons as a maximally entangled state $|\Psi^+\rangle_{AB}$ [Fig. 4(a)], while Alice holds another unknown input qubit $|\phi\rangle_C$ (IN) she wishes to teleport to Bob. (This qubit could be generated by a single-photon source, and perhaps frequency-converted to the telecom band; we refer the reader to Refs. [175–177] for introductions to single-photon source technology.) Alice measures her part of the entangled state (photon A) and the input qubit (photon C) in the Bell basis with a Bell state analyzer (BSA) [Fig. 4(c)], and upon successful detection, transmits the measurement outcomes to Bob through a classical communication channel. Finally, Bob retrieves his half of the entangled pair (photon B) that he had previously stored in a quantum memory [Fig. 1(d)] and applies a unitary operation [Fig. 1(e)] selected based on Alice's measurement outcomes, teleporting the arbitrary input state $|\phi\rangle_C$ to his qubit as $|\phi\rangle_B$ (OUT).

1. Entangled Photon Sources

To contextualize the scheme within frequency-bin encoding, we consider the preshared photon pair state in the Fock basis as $|\Psi^+_{AB}\rangle \propto |1_{A_0} 1_{B_1}\rangle + |1_{A_1} 1_{B_0}\rangle$, while the input qubit $|\phi\rangle$ is expressed as $|\phi\rangle_C = \alpha|1_{C_0}\rangle + \beta|1_{C_1}\rangle$, where $\{A_0, A_1, B_0, B_1, C_0, C_1\}$ represent six computational modes on the frequency

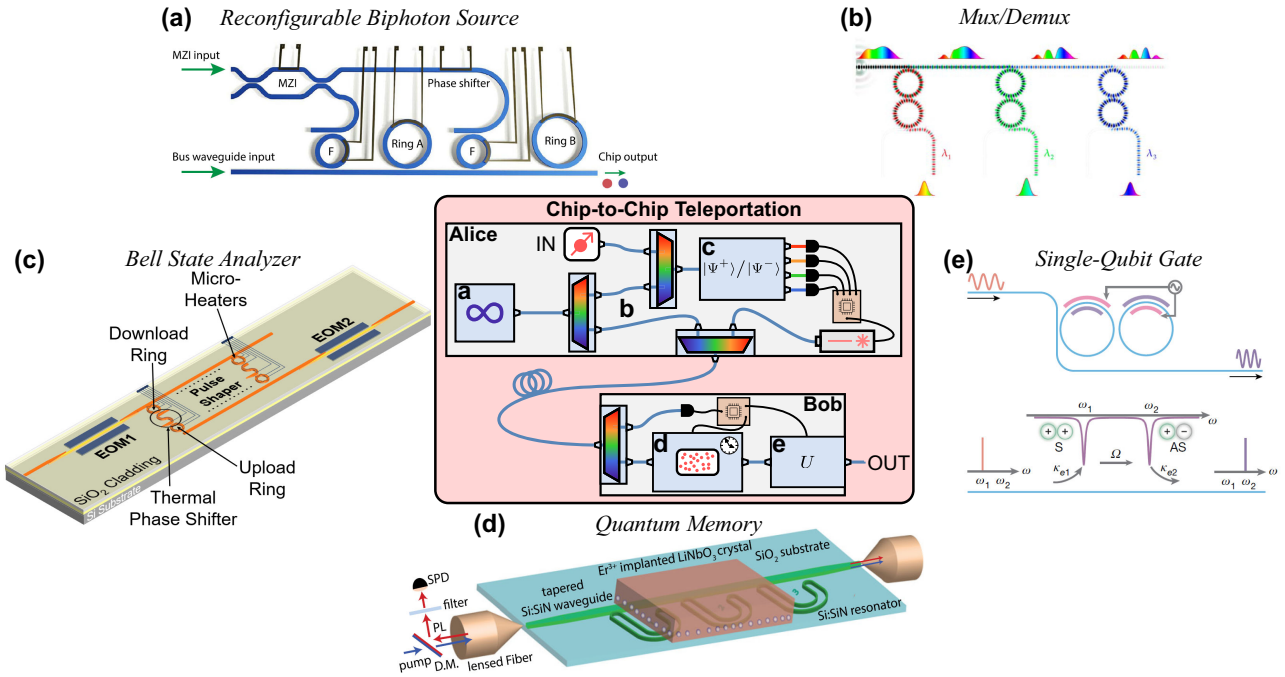

Fig. 4. Envisioned integrated quantum teleportation circuit for frequency qubits. (a)–(e) Architectures proposed to realize the corresponding functionality depicted in the central schematic. (a) Reconfigurable biphoton sources make use of coherently pumped multiple resonators [46]. (b) MRR-based wavelength-division multiplexer [171]. (c) On-chip EOMs and MRR-based pulse shapers (QFP) [172]. (d) Integration of Er:LN crystal with SiN ring resonators [173]. (e) On-chip electro-optic tunable beam splitters based on dynamically modulated ring resonators [174]. Images reproduced with permission from IEEE [172], AIP Publishing [173], Springer Nature [174], an Optica Publishing Group Open Access License [171], and a Creative Commons Attribution 4.0 International License (https://creativecommons.org/licenses/by/4.0/) [46].

grid, in which up to one photon is present. In frequency bins, we have the flexibility to place these modes in a way that is most compatible with subsequent operations [64,65]. Such flexibility, however, might be unattainable for photon sources based on a single nonlinear medium, where the bin spacing is strictly fixed by the resonator's FSR. Accordingly, we advocate for the concept introduced in Section 3.A [149], which utilizes the coherent pumping of multiple cascaded microring resonators (MRRs) for controllable bin-by-bin synthesis. The specific configuration depicted in Fig. 4(a) generates a coherent superposition of two nondegenerate frequency-bin pairs from the first and second rings [46,148] where the qubit bin spacing is determined by the FSR *difference*, which allows for the generation of high-flux entangled states even at tight spacing (<25 GHz). This scheme can be extended to additional MRRs (with identical or distinct FSRs) to produce tunable qudit ($d > 2$) states as well [47]. Exploring the integration of classical frequency comb generators with quantum frequency sources like the above—perhaps drawing on recent work combining a CW pump laser with a quantum frequency comb via hybrid photonics [147]—could make a spectrally tunable, state-reconfigurable, and high-dimensional frequency-bin-entangled source possible on a single chip.

2. Routing and Storage

In the concept of Fig. 4, photon B is sent to Bob's chip, while photon A is combined with the input qubit C. In a tabletop experiment, multiple frequency modes can be combined or separated using DWDM (de)multiplexers or WSSs to direct them to their respective processing units. Nevertheless, MRR filters are more viable options for wavelength management in integrated photonics [178,179]. The resonances of each MRR can be precisely tuned to dynamically match the desired frequency modes. Moreover, to further suppress the crosstalk between adjacent channels, high-order MRRs (i.e., multiple MRRs per frequency channel) can be introduced to realize more box-like filter responses [180,181]. As a result, a multichannel high-order MRR filterbank [171] [Fig. 4(b)] should be able to address tightly spaced frequency modes in a reconfigurable fashion.

Upon arrival at Bob's chip, photon B will ideally be stored in a quantum memory and await the communication of the Bell measurement outcome. Although storage and retrieval of a frequency-bin qubit have not yet been demonstrated experimentally, atomic frequency combs [143,182–184], gradient-echo memories [185–187], and quantum dots [188] have been proposed as possible candidates for storing frequency-bin quantum states. Coupled with progress in integrating quantum memories with nanophotonics, such as rare-earth-doped materials in a nanocavity [173,189,190]—the example highlighted in Fig. 4(d)—the development of such memories would make a complete quantum processing system based on frequency qudits feasible. In any case, it will be critical to align the spectral content of the frequency-bin qudit with the acceptance bandwidth of the memory in question, in terms of both the individual bin width and the total frequency spread. Spectral compression techniques [121,191–194] could therefore prove quite useful for realizing a memory bridging the potentially disparate bandwidths ideal for DWDM transmission and those for atomic storage.

3. State Manipulation

Tabletop QFPs have demonstrated high-fidelity single- and two-qubit operations, such as the BSA [65] and single-qubit rotations [155] for teleportation. However, fully integrated QFPs have the potential to overcome limitations seen in tabletop setups, such as high insertion loss—typically 2–3 dB and 4–5 dB for commercial EOMs [195,196] and pulse shapers [197], respectively—and limited spectral resolution ($\gtrsim$10 GHz). Figure 4(c) illustrates the vision for such a device [172,198], which consists of a pair of integrated EOMs bookending an MRR-based pulse shaper. On-chip EOMs with low loss and large-scale photonic integration have been a persistent challenge in traditional silicon photonics, given the absence of an efficient electro-optic effect. Plasma dispersion modulators have emerged as an alternative [199–201], but their inherent loss limits their suitability for quantum applications. However, recent advances in thin-film lithium niobate [202,203], CMOS-compatible silicon-organic hybrid platforms [204–206], and III-V materials like (Al)GaAs [207,208] and InP [209,210] offer promising opportunities for achieving high-speed integrated modulators with low loss (<1 dB). In terms of pulse shaping, the proposed design draws inspiration from previous classical demonstrations [211–213], leveraging MRR filters for channel add–drop operations and microheaters for phase shifts. Each pulse shaper channel employs an MRR filter to download a single frequency mode from the input waveguide, followed by a thermo-optic phase shifter for the desired phase adjustment. Finally, another MRR filter uploads the shaped frequency mode back to the common output waveguide. More sophisticated designs, such as high-order MRRs and racetrack-based filters [214,215], can further narrow the filter passbands (and thus, the bin separation) to a few GHz without significant loss (<1 dB), even with commercial foundries [216,217]. As estimated by a recent theoretical study [172], current technology should enable the fabrication of a CMOS QFP comprising two EOMs and one pulse shaper with only ∼5 dB total loss, compared to the 12.5 dB previously observed with discrete fiber-optic components [61].

In the pursuit of integrated QFPs, the focus lies on the on-chip realization of key components, namely, EOMs and pulse shapers, by exploring suitable material platforms that can accommodate both functionalities. However, alternative approaches such as coupled-cavity modulators [174,218–220] offer intriguing possibilities, as they have the potential to directly synthesize the target frequency operations directly without a cascade of discrete elements. As an example, Fig. 4(e) shows a coupled-ring system that supports symmetric (S) and anti-symmetric (AS) hybrid modes. By applying sinusoidal microwave signals to the resonators, with frequencies matching the two-mode splitting, energy transfer between the modes can be achieved, effectively forming a tunable frequency beamsplitter. This enables the synthesis of arbitrary two-dimensional unitaries for frequency qubits by adjusting the microwave power and phase accordingly, making such a device well suited to the unitary feedforward step concluding the teleportation protocol of Fig. 4.

4. RF Synchronization

All frequency-bin experiments so far have been performed under local conditions in a single laboratory. In the case of electro-optic gates, for example, this means that all EOMs have enjoyed access to a single RF source distributed through comparatively short cables, thus maintaining EOM-to-EOM jitters at levels sufficiently low that they have produced no noticeable reduction on experimental fidelities. Yet for the distributed communications and networking tasks envisioned in the future of frequency-bin QIP—of which the chip-to-chip teleportation in Fig. 4 is an example—some RF reference must be shared across communicating nodes to ensure a constant phase relationship between operations performed nonlocally on the photonic state. A large body of work in fiber-optic time and frequency transfer [221–223] offers a foundation that could be leveraged for frequency-bin QIP as well, and commercial open-source options like White Rabbit [224–227] have demonstrated jitters as low as 1.1 ps root-mean-square from 1–30 Hz (0.8 ps from 100–10,000 Hz) over a 10 km fiber spool [225].

For frequency bins, the spacing $\Delta\omega$ implies that the node-to-node RF jitter $\Delta\tau$ should satisfy $\Delta\tau \ll 2\pi/\Delta\omega$. However, quantitative tolerances for specific operations (fidelity versus $\Delta\tau$) have not been developed, leaving important open questions regarding the RF synchronization architecture that will ultimately be required for distributed frequency-bin processing. In particular, the disparity in the cost and complexity of (i) as- and fs-scale-jitter time transfer with frequency combs and active link stabilization [221,223], (ii) sub-ps nonlocal delay sensing with entangled photons [169], (iii) few ps-scale jitter with White Rabbit [224,225], and (iv) custom analog photonic links that might lie anywhere along this spectrum [228] suggests a variety of potential futures for scaling up frequency-bin quantum networking. Further analysis and experimental tests on the jitter question will therefore prove critical as this field continues to progress.

B. Quantum Interconnects

Interestingly, one of the original motivations for the QFP was the development of quantum interconnects for spectrally heterogeneous matter qubits [7]—a promising frequency-bin application that has yet to be fully realized. A quantum interconnect aims to entangle physically separated quantum systems that cannot directly interact, forming the basis of several quantum repeater architectures and enabling the transfer of quantum information; for example, the preshared entanglement required in Fig. 4 could be supported by interconnected matter qubits rather than entangled photons, a situation valuable for unconditional teleportation where each input state $|\phi\rangle_C$ is teleported with unit success [229,230]. While matter qubits are proficient in serving as quantum memories and computing modules, photons play a unique role as quantum information carriers, particularly in long-distance networks. A crucial component of photonic-based matter qubit interconnects is the entanglement swapping operation. First, photons are generated by exciting a matter qubit system in such a way that the photon and matter qubit are entangled; e.g., the matter qubit could exist in a coherent superposition of two levels, where each level corresponds to some property of the emitted photon, polarization being an archetypal example [231]. Then, photons from two such systems can be brought together at a third location, interfered, and measured in such a way to erase their origin information. Through successful measurement, the initially local entanglement is transferred to distant matter qubits. Depending on the number of photons detected in the process [232,233], most examples can be classified into type-I (Duan–Lukin–Cirac–Zoller [234]) and type-II protocols [231,235,236]. Both protocols typically require photons with identical frequencies, which can be

challenging to achieve for dissimilar matter qubits or qubits in different local environments.

In this section, we discuss how a QFP could effectively manage this frequency mismatch by implementing the required frequency-bin operations for both type-I and type-II quantum interconnects. Such processing units may also prove useful for spectrally multiplexed quantum memories and networks [182,183]. One overarching challenge of note is the general disparity in the emission wavelengths of typical matter systems (∼800 nm) and state-of-the-art frequency-bin sources that, as highlighted in Table 1, are dominated by C-band solutions (∼1550 nm). Because the pull between the spectral bands convenient for emitters and for fiber-optic communications is not unique to frequency-bin encoding but shared by quantum networking with any photonic DoF, we do not focus on this challenge specifically here; solutions such as interband quantum frequency conversion [86,87,170] are well-known and active areas of research. And although relatively uncommon, explicit frequency-bin-entangled sources directly compatible with atomic memories have been demonstrated [128,129], indicating another profitable direction for frequency-bin interfacing with matter systems.

1. Type-I Interconnect

In the original type-I paradigm [234], two separated matter qubits, such as atomic ensembles in a lambda-type three-level configuration, are coherently excited by a weak write pulse, leading to a low probability of photon emission. To entangle the matter qubits, the emitted modes are brought to a 50/50 spatial beamsplitter for interference. Ideally, successful detection of *one photon* projects the ensembles onto an entangled state. However, in the presence of frequency mismatch, it becomes necessary to introduce a frequency shifter or beamsplitter to eliminate the spectral distinguishability between the two photons. Notably, in an early demonstration [237] preceding even the advent of the term "frequency bin," entanglement between two distinct atomic species was achieved using a single EOM to implement what amounts to a probabilistic frequency Hadamard operation. Similarly, Ref. [182] employed an EOM, this time through serrodyne modulation, to realize frequency-selective recall from a multimode quantum memory. We anticipate that the frequency beamsplitters illustrated in Fig. 2 will be valuable in both of these scenarios.

In addition, a type-I interconnect can be extended to generate W-state [238] entanglement of $d > 2$ qubits, where a single excitation is shared among d spatially distinct ensembles. This capability was initially demonstrated in path encoding [239,240], where a multimode interferometer, consisting of a cascade of beamsplitters and phase shifters, coherently mixed $d = 4$ spatial modes together. However, the scalability of the path-encoding scheme is hindered by the strict requirements on optical phase stability, including both fiber links and pump lasers, across all distant systems. Instead, we envisage a modified scheme based on spectral encoding, as depicted in Fig. 5(a). In this scheme, we assume that all d emission frequencies are disparate and tuned to one line in a $\Delta\omega$-spaced grid. The nodes are collinearly coupled to a single fiber-optic spatial mode, enabling interferometric stability as path length fluctuations are shared by all bins. By propagating a single pump pulse through the network, we can prepare an output state consisting of a single-photon excitation in a polychromatic superposition of all d frequencies, entangled with each matter qubit. To coherently mix all the frequency modes, we can employ the discrete Fourier transform (DFT) denoted by the matrix elements $U_{kj} = d^{-1/2}\exp(2\pi ikj/d)$ $(k, j \in \{0, 1, \ldots, d-1\})$. If we assume for concreteness that the photonic–matter state is prepared in an equiamplitude, in-phase superposition, then post-DFT detection of a photon at frequency ω_k will herald the entangled W-like matter state $|\psi_k\rangle = \sum_{j=0}^{d-1} U_{kj}|0\cdots 01_j 0\cdots 0\rangle$, where each term signifies a single qubit j occupying logical $|1\rangle$ [defined as the lowest energy level in the lambda scheme in Fig. 5(a)].

The use of DFT operations in frequency bins is especially intriguing due to its promising scaling. For example, a three-element QFP can realize a d-dimensional DFT without the need for additional components such as pulse shapers or EOMs: rather, the synthesis of one additional RF tone per dimension d is sufficient, as demonstrated in simulations up to $d = 10$ [131]. Furthermore, tabletop QFPs have already demonstrated high-fidelity three-dimensional frequency DFT gates, also known as frequency tritters [61,131]. With future integrated QFPs attaining tighter spacings $\Delta\omega$, such as that discussed in Section 4.A.3, it will therefore be possible to support higher-dimensional operations under a fixed RF bandwidth, as the d-point DFT under this construction requires a maximum RF frequency proportional to both d and $\Delta\omega$: $(d-1)\Delta\omega$ [131].

2. Type-II Interconnect

Type-II interconnects have been proposed for matter qubits that exhibit strong coupling to photons, including cold atoms and ions [231,235,236]. In contrast to type-I protocols, type-II protocols involve the excitation of matter qubits with near-unity probability, resulting in their quantum state becoming entangled with an emitting photon that carries a qubit in two orthogonal modes, such as polarization encoding with H/V states. The successful transfer of entanglement to two distant matter qubits relies on entanglement swapping operations that require the coincidence detection of *two photons* [241,242], typically accomplished using a BSA. However, conventional BSAs require that the photons be spectrally indistinguishable, as any frequency mismatch can potentially project the matter qubits onto a mixed state. Proposed techniques to mitigate these effects include time-resolved detection followed by active feed-forward operations [243,244], but their effectiveness is ultimately limited by the temporal resolution of photon detection.

On the other hand, frequency qubits, which naturally complement matter qubits like trapped ions [245], have historically been overlooked due to the challenges associated with their manipulation and control. However, the progress outlined in this mini-review suggests that the potential of frequency qubits can finally be unlocked and applied to type-II interconnects as well. For example, consider the scenario of two identical ion trap systems where emitting photons are frequency-encoded and share the *same* spectral content. Here, entanglement swapping can be achieved by mixing two photons at a spatial beamsplitter, followed by spectrally resolved detections [140]. In more general cases where slight differences in frequency transitions exist between the matter systems [Fig. 5(b)], the participating photons consist of four frequency modes: $\{\omega_A, \omega_A + \Delta\omega\}$ from system A, and $\{\omega_B, \omega_B + \Delta\omega\}$ from system B. To address this situation, a solution based on frequency mixing can be employed, utilizing two parallel, interleaved frequency beamsplitters to enable high-fidelity Bell state measurements. Notably, these capabilities have already been demonstrated on QFP circuits [65], highlighting

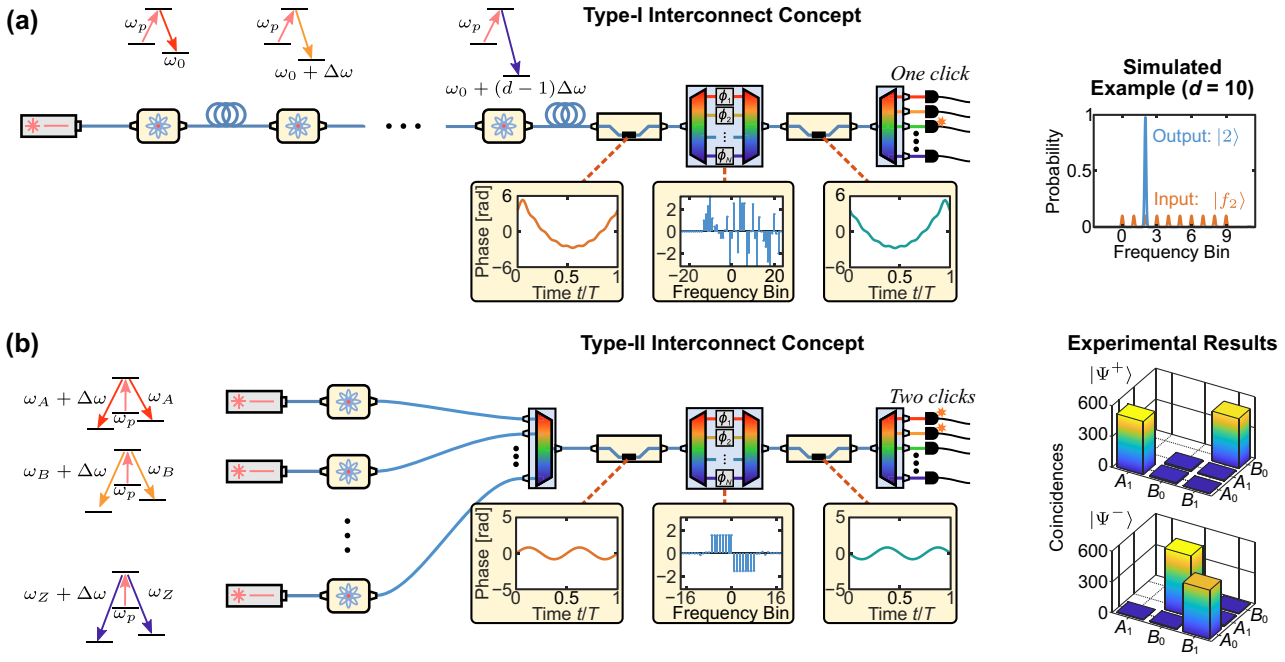

Fig. 5. Vision for frequency-bin quantum interconnects. (a) Type I. Spectrally tuned sources are excited by a copropagating pump laser, and the output is sent through a QFP performing a d-point DFT ($d = 10$ solution shown) [131]. The detection of a single photon heralds a d-dimensional W state. (b) Type II. Sources emitting true frequency-bin qubits are multiplexed and fed into a frequency-bin BSA. A coincidence signifies that two matter qubits have been entangled, with a specific state determined by the frequencies observed [65].

the potential of frequency qubits in facilitating efficient interconnects and entanglement operations. Unlike the type-I design, type-II interconnects do not require subwavelength phase stability (only that the interfering photons temporally overlap), so we have not depicted the spectral version in Fig. 5(b) with matter qubits coupled to a single waveguide, although such a configuration is certainly possible. In the type-II case, the primary value of frequency-bin encoding emerges in the BSA operation, which can be realized in parallel on multiple pairs of qubits simultaneously in a single QFP and—subject to electro-optic bandwidth limitations—can even be reconfigured to entangle different pairs on demand through modifications to the drive frequency.

5. CONCLUSION

Tools for frequency-bin QIP have advanced rapidly over the last few years, transforming frequency qubits from a scientific curiosity into a practicable platform for quantum information. The trends in sources, gates, and detection schemes outlined in this mini-review point to a promising future in quantum communications and networking. And while we have focused on photonic integration and spectrally multiplexed interconnects as particularly auspicious directions for future development, other applications in quantum networking appear ripe for frequency-bin encoding, such as nonlocal delay sensing [169] and quantum key distribution [246–249]. Moreover, irrespective of the level of adoption of full frequency-bin *encoding* in future quantum networks, frequency *multiplexing* will likely prove critical for scalability within a heavily subscribed fiber-optic infrastructure, as already suggested by entanglement distribution experiments [226,250–256] leveraging frequency-multiplexed polarization entanglement and many of the same tools (sources, WSSs) required for full frequency-bin encoding. Accordingly, we are excited to see how the perception and utilization of frequency bins may continue to evolve, and we hope this review will inspire more researchers to enter and accelerate this exciting field.

Funding. Ministero dell'Università e della Ricerca (PE0000023-NQSTI); National Science Foundation (ECCS-2034019, PHY-2110615); Air Force Research Laboratory (FA8750-20-P-1705); U.S. Department of Energy, Office of Science, National Quantum Information Science Research Centers, Co-design Center for Quantum Advantage (C2QA); U.S. Department of Energy, Office of Science, Advanced Scientific Computing Research (ERKJ353, ERKJ381).

Acknowledgment. The authors would like to thank S. Fatema for valuable discussions. A portion of this work was performed at Oak Ridge National Laboratory, operated by UT-Battelle for the U.S. Department of Energy. The Quantum Collaborative, led by Arizona State University, provided valuable expertise and resources for this work.

Disclosures. The authors declare no conflicts of interest.

Data availability. No data were generated or analyzed in the presented research.

REFERENCES

1. E. Agrell, M. Karlsson, A. R. Chraplyvy, *et al.*, "Roadmap of optical communications," J. Opt. **18**, 063002 (2016).
2. M. A. Khalighi and M. Uysal, "Survey on free space optical communication: a communication theory perspective," Commun. Surveys Tuts. **16**, 2231–2258 (2014).
3. M. Kues, C. Reimer, J. M. Lukens, *et al.*, "Quantum optical microcombs," Nat. Photonics **13**, 170–179 (2019).
4. H.-H. Lu, A. M. Weiner, P. Lougovski, *et al.*, "Quantum information processing with frequency-comb qudits," IEEE Photon. Technol. Lett. **31**, 1858–1861 (2019).
5. S. Sciara, C. Reimer, M. Kues, *et al.*, "Universal N-partite d-level pure-state entanglement witness based on realistic measurement settings," Phys. Rev. Lett. **122**, 120501 (2019).
6. H.-H. Lu, N. A. Peters, A. M. Weiner, *et al.*, "Characterization of quantum frequency processors," IEEE J. Sel. Top. Quantum Electron. **29**, 6300112 (2023).

7. J. M. Lukens and P. Lougovski, "Frequency-encoded photonic qubits for scalable quantum information processing," Optica **4**, 8–16 (2017).
8. N. C. Menicucci, S. T. Flammia, and O. Pfister, "One-way quantum computing in the optical frequency comb," Phys. Rev. Lett. **101**, 130501 (2008).
9. M. Pysher, Y. Miwa, R. Shahrokhshahi, *et al.*, "Parallel generation of quadripartite cluster entanglement in the optical frequency comb," Phys. Rev. Lett. **107**, 030505 (2011).
10. J. Roslund, R. M. de Araújo, S. Jiang, *et al.*, "Wavelength-multiplexed quantum networks with ultrafast frequency combs," Nat. Photonics **8**, 109–112 (2014).
11. M. Chen, N. C. Menicucci, and O. Pfister, "Experimental realization of multipartite entanglement of 60 modes of a quantum optical frequency comb," Phys. Rev. Lett. **112**, 120505 (2014).
12. O. Pfister, "Continuous-variable quantum computing in the quantum optical frequency comb," J. Phys. B **53**, 012001 (2020).
13. X. Zhu, C.-H. Chang, C. González-Arciniegas, *et al.*, "Hypercubic cluster states in the phase-modulated quantum optical frequency comb," Optica **8**, 281–290 (2021).
14. B. Brecht, A. Eckstein, A. Christ, *et al.*, "From quantum pulse gate to quantum pulse shaper—engineered frequency conversion in nonlinear optical waveguides," New J. Phys. **13**, 065029 (2011).
15. B. Brecht, A. Eckstein, R. Ricken, *et al.*, "Demonstration of coherent time-frequency Schmidt mode selection using dispersion-engineered frequency conversion," Phys. Rev. A **90**, 030302 (2014).
16. B. Brecht, D. V. Reddy, C. Silberhorn, *et al.*, "Photon temporal modes: a complete framework for quantum information science," Phys. Rev. X **5**, 041017 (2015).
17. P. Manurkar, N. Jain, M. Silver, *et al.*, "Multidimensional mode-separable frequency conversion for high-speed quantum communication," Optica **3**, 1300–1307 (2016).
18. D. V. Reddy and M. G. Raymer, "High-selectivity quantum pulse gating of photonic temporal modes using all-optical Ramsey interferometry," Optica **5**, 423–428 (2018).
19. V. Ansari, J. M. Donohue, M. Allgaier, *et al.*, "Tomography and purification of the temporal-mode structure of quantum light," Phys. Rev. Lett. **120**, 213601 (2018).
20. V. Ansari, J. M. Donohue, B. Brecht, *et al.*, "Tailoring nonlinear processes for quantum optics with pulsed temporal-mode encodings," Optica **5**, 534–550 (2018).
21. M. G. Raymer and I. A. Walmsley, "Temporal modes in quantum optics: then and now," Phys. Scr. **95**, 064002 (2020).
22. M. Karpiński, A. O. C. Davis, F. Sośnicki, *et al.*, "Control and measurement of quantum light pulses for quantum information science and technology," Adv. Quantum Technol. **4**, 2000150 (2021).
23. S. E. Harris, M. K. Oshman, and R. L. Byer, "Observation of tunable optical parametric fluorescence," Phys. Rev. Lett. **18**, 732–734 (1967).
24. D. C. Burnham and D. L. Weinberg, "Observation of simultaneity in parametric production of optical photon pairs," Phys. Rev. Lett. **25**, 84–87 (1970).
25. L. Mandel and E. Wolf, *Optical Coherence and Quantum Optics* (Cambridge University, 1995).
26. Y. Shih, "Entangled biphoton source—property and preparation," Rep. Prog. Phys. **66**, 1009–1044 (2003).
27. S. Tanzilli, H. De Riedmatten, W. Tittel, *et al.*, "Highly efficient photon-pair source using periodically poled lithium niobate waveguide," Electron. Lett. **37**, 26–28 (2001).
28. S. Tanzilli, W. Tittel, H. De Riedmatten, *et al.*, "PPLN waveguide for quantum communication," Eur. Phys. J. D **18**, 155–160 (2002).
29. M. Fiorentino, S. M. Spillane, R. G. Beausoleil, *et al.*, "Spontaneous parametric down-conversion in periodically poled KTP waveguides and bulk crystals," Opt. Express **15**, 7479–7488 (2007).
30. W. P. Grice, A. B. U'Ren, and I. A. Walmsley, "Eliminating frequency and space-time correlations in multiphoton states," Phys. Rev. A **64**, 063815 (2001).
31. P. J. Mosley, J. S. Lundeen, B. J. Smith, *et al.*, "Heralded generation of ultrafast single photons in pure quantum states," Phys. Rev. Lett. **100**, 133601 (2008).
32. C. Chen, C. Bo, M. Y. Niu, *et al.*, "Efficient generation and characterization of spectrally factorable biphotons," Opt. Express **25**, 7300–7312 (2017).
33. Z. Vernon, M. Menotti, C. C. Tison, *et al.*, "Truly unentangled photon pairs without spectral filtering," Opt. Lett. **42**, 3638–3641 (2017).
34. Y. J. Lu, R. L. Campbell, and Z. Y. Ou, "Mode-locked two-photon states," Phys. Rev. Lett. **91**, 163602 (2003).
35. A. Zavatta, S. Viciani, and M. Bellini, "Recurrent fourth-order interference dips and peaks with a comblike two-photon entangled state," Phys. Rev. A **70**, 023806 (2004).
36. M. A. Sagioro, C. Olindo, C. H. Monken, *et al.*, "Time control of two-photon interference," Phys. Rev. A **69**, 053817 (2004).
37. Z. Xie, T. Zhong, S. Shrestha, *et al.*, "Harnessing high-dimensional hyperentanglement through a biphoton frequency comb," Nat. Photonics **9**, 536–542 (2015).
38. G. Maltese, M. I. Amanti, F. Appas, *et al.*, "Generation and symmetry control of quantum frequency combs," npj Quantum Inf. **6**, 13 (2020).
39. Z. Y. Ou and Y. J. Lu, "Cavity enhanced spontaneous parametric down-conversion for the prolongation of correlation time between conjugate photons," Phys. Rev. Lett. **83**, 2556–2559 (1999).
40. H. Goto, Y. Yanagihara, H. Wang, *et al.*, "Observation of an oscillatory correlation function of multimode two-photon pairs," Phys. Rev. A **68**, 015803 (2003).
41. H. Goto, H. Wang, T. Horikiri, *et al.*, "Two-photon interference of multimode two-photon pairs with an unbalanced interferometer," Phys. Rev. A **69**, 035801 (2004).
42. C. L. Morrison, F. Graffitti, P. Barrow, *et al.*, "Frequency-bin entanglement from domain-engineered down-conversion," APL Photon. **7**, 066102 (2022).
43. S. Clemmen, K. P. Huy, W. Bogaerts, *et al.*, "Continuous wave photon pair generation in silicon-on-insulator waveguides and ring resonators," Opt. Express **17**, 16558–16570 (2009).
44. S. Azzini, D. Grassani, M. J. Strain, *et al.*, "Ultra-low power generation of twin photons in a compact silicon ring resonator," Opt. Express **20**, 23100–23107 (2012).
45. D. Grassani, S. Azzini, M. Liscidini, *et al.*, "Micrometer-scale integrated silicon source of time-energy entangled photons," Optica **2**, 88–94 (2015).
46. M. Clementi, F. A. Sabattoli, M. Borghi, *et al.*, "Programmable frequency-bin quantum states in a nano-engineered silicon device," Nat. Commun. **14**, 176 (2023).
47. M. Borghi, N. Tagliavacche, F. A. Sabattoli, *et al.*, "Reconfigurable silicon photonic chip for the generation of frequency-bin-entangled qudits," Phys. Rev. Appl. **19**, 064026 (2023).
48. C. Reimer, L. Caspani, M. Clerici, *et al.*, "Integrated frequency comb source of heralded single photons," Opt. Express **22**, 6535–6546 (2014).
49. C. Reimer, M. Kues, P. Roztocki, *et al.*, "Generation of multiphoton entangled quantum states by means of integrated frequency combs," Science **351**, 1176–1180 (2016).
50. M. Kues, C. Reimer, P. Roztocki, *et al.*, "On-chip generation of high-dimensional entangled quantum states and their coherent control," Nature **546**, 622–626 (2017).
51. P. Roztocki, M. Kues, C. Reimer, *et al.*, "Practical system for the generation of pulsed quantum frequency combs," Opt. Express **25**, 18940–18949 (2017).
52. K. Sugiura, Z. Yin, R. Okamoto, *et al.*, "Broadband generation of photon-pairs from a CMOS compatible device," Appl. Phys. Lett. **116**, 224001 (2020).
53. S. Ramelow, A. Farsi, S. Clemmen, *et al.*, "Silicon-nitride platform for narrowband entangled photon generation," arXiv, arXiv:1508.04358 (2015).
54. J. A. Jaramillo-Villegas, P. Imany, O. D. Odele, *et al.*, "Persistent energy–time entanglement covering multiple resonances of an on-chip biphoton frequency comb," Optica **4**, 655–658 (2017).
55. P. Imany, J. A. Jaramillo-Villegas, O. D. Odele, *et al.*, "50-GHz-spaced comb of high-dimensional frequency-bin entangled photons from an on-chip silicon nitride microresonator," Opt. Express **26**, 1825–1840 (2018).
56. C. Joshi, A. Farsi, A. Dutt, *et al.*, "Frequency-domain quantum interference with correlated photons from an integrated microresonator," Phys. Rev. Lett. **124**, 143601 (2020).
57. H.-H. Lu, K. V. Myilswamy, R. S. Bennink, *et al.*, "Bayesian tomography of high-dimensional on-chip biphoton frequency combs with randomized measurements," Nat. Commun. **13**, 4338 (2022).
58. T. J. Steiner, J. E. Castro, L. Chang, *et al.*, "Ultrabright entangled-photon-pair generation from an AlGaAs-on-insulator microring resonator," PRX Quantum **2**, 010337 (2021).

59. L. Zhang, C. Cui, J. Yan, *et al.*, "On-chip parallel processing of quantum frequency comb," npj Quantum Inf. **9**, 57 (2023).
60. S. Clemmen, A. Farsi, S. Ramelow, *et al.*, "Ramsey interference with single photons," Phys. Rev. Lett. **117**, 223601 (2016).
61. H.-H. Lu, J. M. Lukens, N. A. Peters, *et al.*, "Electro-optic frequency beam splitters and tritters for high-fidelity photonic quantum information processing," Phys. Rev. Lett. **120**, 030502 (2018).
62. L. G. Helt, Z. Yang, M. Liscidini, *et al.*, "Spontaneous four-wave mixing in microring resonators," Opt. Lett. **35**, 3006–3008 (2010).
63. H.-H. Lu, J. M. Lukens, N. A. Peters, *et al.*, "Quantum interference and correlation control of frequency-bin qubits," Optica **5**, 1455–1460 (2018).
64. H.-H. Lu, J. M. Lukens, B. P. Williams, *et al.*, "A controlled-NOT gate for frequency-bin qubits," npj Quantum Inf. **5**, 24 (2019).
65. N. B. Lingaraju, H.-H. Lu, D. E. Leaird, *et al.*, "Bell state analyzer for spectrally distinct photons," Optica **9**, 280–283 (2022).
66. A. K. Kashi and M. Kues, "Spectral Hong–Ou–Mandel interference between independently generated single photons for scalable frequency-domain quantum processing," Laser Photon. Rev. **15**, 2000464 (2021).
67. K. V. Myilswamy, S. Seshadri, H.-H. Lu, *et al.*, "Time-resolved Hanbury Brown–Twiss interferometry of on-chip biphoton frequency combs using Vernier phase modulation," Phys. Rev. Appl. **19**, 034019 (2023).
68. A. M. Weiner, "Femtosecond pulse shaping using spatial light modulators," Rev. Sci. Instrum. **71**, 1929–1960 (2000).
69. A. M. Weiner, "Ultrafast optical pulse shaping: a tutorial review," Opt. Commun. **284**, 3669–3692 (2011).
70. A. Pe'er, B. Dayan, A. A. Friesem, *et al.*, "Temporal shaping of entangled photons," Phys. Rev. Lett. **94**, 073601 (2005).
71. B. Dayan, Y. Bromberg, I. Afek, *et al.*, "Spectral polarization and spectral phase control of time-energy entangled photons," Phys. Rev. A **75**, 043804 (2007).
72. F. Zäh, M. Halder, and T. Feurer, "Amplitude and phase modulation of time-energy entangled two-photon states," Opt. Express **16**, 16452–16458 (2008).
73. E. Poem, Y. Gilead, Y. Lahini, *et al.*, "Fourier processing of quantum light," Phys. Rev. A **86**, 023836 (2012).
74. C. Bernhard, B. Bessire, T. Feurer, *et al.*, "Shaping frequency-entangled qudits," Phys. Rev. A **88**, 032322 (2013).
75. B. Bessire, C. Bernhard, T. Feurer, *et al.*, "Versatile shaper-assisted discretization of energy-time entangled photons," New J. Phys. **16**, 033017 (2014).
76. S. Schwarz, B. Bessire, A. Stefanov, *et al.*, "Bipartite Bell inequalities with three ternary-outcome measurements—from theory to experiments," New J. Phys. **18**, 035001 (2016).
77. J. M. Lukens, A. Dezfooliyan, C. Langrock, *et al.*, "Biphoton manipulation with a fiber-based pulse shaper," Opt. Lett. **38**, 4652–4655 (2013).
78. J. M. Lukens, A. Dezfooliyan, C. Langrock, *et al.*, "Demonstration of high-order dispersion cancellation with an ultrahigh-efficiency sum-frequency correlator," Phys. Rev. Lett. **111**, 193603 (2013).
79. J. M. Lukens, A. Dezfooliyan, C. Langrock, *et al.*, "Orthogonal spectral coding of entangled photons," Phys. Rev. Lett. **112**, 133602 (2014).
80. J. M. Lukens, O. Odele, C. Langrock, *et al.*, "Generation of biphoton correlation trains through spectral filtering," Opt. Express **22**, 9585–9596 (2014).
81. O. D. Odele, J. M. Lukens, J. A. Jaramillo-Villegas, *et al.*, "Tunable delay control of entangled photons based on dispersion cancellation," Opt. Express **23**, 21857–21866 (2015).
82. Z. Jiang, D. S. Seo, D. E. Leaird, *et al.*, "Spectral line-by-line pulse shaping," Opt. Lett. **30**, 1557–1559 (2005).
83. F. Ferdous, H. Miao, D. E. Leaird, *et al.*, "Spectral line-by-line pulse shaping of on-chip microresonator frequency combs," Nat. Photonics **5**, 770–776 (2011).
84. C. Cui, K. P. Seshadreesan, S. Guha, *et al.*, "High-dimensional frequency-encoded quantum information processing with passive photonics and time-resolving detection," Phys. Rev. Lett. **124**, 190502 (2020).
85. C. J. McKinstrie, S. Radic, and M. Raymer, "Quantum noise properties of parametric amplifiers driven by two pump waves," Opt. Express **12**, 5037–5066 (2004).
86. P. Kumar, "Quantum frequency conversion," Opt. Lett. **15**, 1476–1478 (1990).
87. J. Huang and P. Kumar, "Observation of quantum frequency conversion," Phys. Rev. Lett. **68**, 2153–2156 (1992).
88. M. A. Albota and F. N. C. Wong, "Efficient single-photon counting at 1.55 μm by means of frequency upconversion," Opt. Lett. **29**, 1449–1451 (2004).
89. C. Langrock, E. Diamanti, R. V. Roussev, *et al.*, "Highly efficient single-photon detection at communication wavelengths by use of upconversion in reverse-proton-exchanged periodically poled $LiNbO_3$ waveguides," Opt. Lett. **30**, 1725–1727 (2005).
90. S. Tanzilli, W. Tittel, M. Halder, *et al.*, "A photonic quantum information interface," Nature **437**, 116–120 (2005).
91. J. S. Pelc, L. Ma, C. R. Phillips, *et al.*, "Long-wavelength-pumped upconversion single-photon detector at 1550 nm: performance and noise analysis," Opt. Express **19**, 21445–21456 (2011).
92. R. Ikuta, Y. Kusaka, T. Kitano, *et al.*, "Wide-band quantum interface for visible-to-telecommunication wavelength conversion," Nat. Commun. **2**, 537 (2011).
93. X. Wang, X. Jiao, B. Wang, *et al.*, "Quantum frequency conversion and single-photon detection with lithium niobate nanophotonic chips," npj Quantum Inf. **9**, 38 (2023).
94. M. Bock, P. Eich, S. Kucera, *et al.*, "High-fidelity entanglement between a trapped ion and a telecom photon via quantum frequency conversion," Nat. Commun. **9**, 1998 (2018).
95. R. Ikuta, T. Kobayashi, T. Kawakami, *et al.*, "Polarization insensitive frequency conversion for an atom-photon entanglement distribution via a telecom network," Nat. Commun. **9**, 1997 (2018).
96. V. Krutyanskiy, M. Meraner, J. Schupp, *et al.*, "Light-matter entanglement over 50km of optical fibre," npj Quantum Inf. **5**, 72 (2019).
97. A. Tchebotareva, S. L. Hermans, P. C. Humphreys, *et al.*, "Entanglement between a diamond spin qubit and a photonic time-bin qubit at telecom wavelength," Phys. Rev. Lett. **123**, 063601 (2019).
98. T. van Leent, M. Bock, R. Garthoff, *et al.*, "Long-distance distribution of atom-photon entanglement at telecom wavelength," Phys. Rev. Lett. **124**, 010510 (2020).
99. N. Maring, P. Farrera, K. Kutluer, *et al.*, "Photonic quantum state transfer between a cold atomic gas and a crystal," Nature **551**, 485–488 (2017).
100. N. Maring, D. Lago-Rivera, A. Lenhard, *et al.*, "Quantum frequency conversion of memory-compatible single photons from 606 nm to the telecom C-band," Optica **5**, 507–513 (2018).
101. Y. Yu, F. Ma, X.-Y. Luo, *et al.*, "Entanglement of two quantum memories via fibres over dozens of kilometres," Nature **578**, 240–245 (2020).
102. T. van Leent, M. Bock, F. Fertig, *et al.*, "Entangling single atoms over 33km telecom fibre," Nature **607**, 69–73 (2022).
103. X.-Y. Luo, Y. Yu, J.-L. Liu, *et al.*, "Postselected entanglement between two atomic ensembles separated by 12.5 km," Phys. Rev. Lett. **129**, 050503 (2022).
104. C. J. McKinstrie, J. D. Harvey, S. Radic, *et al.*, "Translation of quantum states by four-wave mixing in fibers," Opt. Express **13**, 9131–9142 (2005).
105. H. J. McGuinness, M. G. Raymer, C. J. McKinstrie, *et al.*, "Quantum frequency translation of single-photon states in a photonic crystal fiber," Phys. Rev. Lett. **105**, 093604 (2010).
106. C. Joshi, A. Farsi, S. Clemmen, *et al.*, "Frequency multiplexing for quasi-deterministic heralded single-photon sources," Nat. Commun. **9**, 847 (2018).
107. I. Agha, M. Davanço, B. Thurston, *et al.*, "Low-noise chip-based frequency conversion by four-wave-mixing Bragg scattering in SiN_x waveguides," Opt. Lett. **37**, 2997–2999 (2012).
108. Q. Li, M. Davanço, and K. Srinivasan, "Efficient and low-noise single-photon-level frequency conversion interfaces using silicon nanophotonics," Nat. Photonics **10**, 406–414 (2016).
109. A. Singh, Q. Li, S. Liu, *et al.*, "Quantum frequency conversion of a quantum dot single-photon source on a nanophotonic chip," Optica **6**, 563–569 (2019).
110. R. Tyumenev, J. Hammer, N. Y. Joly, *et al.*, "Tunable and state-preserving frequency conversion of single photons in hydrogen," Science **376**, 621–624 (2022).
111. R. Oliver, M. Blau, X. Ji, *et al.*, "Photonic interference beyond two modes," in *Quantum 2.0* (Optica, 2023), paper QW4A.3.
112. C. Joshi, A. Farsi, and A. Gaeta, "Frequency-domain boson sampling," in *Conference on Lasers and Electro-Optics (CLEO)* (Optica Publishinng Group, 2017), paper FTu1F.1.
113. G. L. Li and P. K. L. Yu, "Optical intensity modulators for digital and analog applications," J. Lightwave Technol. **21**, 2010–2030 (2003).

114. P. Kolchin, C. Belthangady, S. Du, *et al.*, "Electro-optic modulation of single photons," Phys. Rev. Lett. **101**, 103601 (2008).
115. C. Belthangady, C.-S. Chuu, I. A. Yu, *et al.*, "Hiding single photons with spread spectrum technology," Phys. Rev. Lett. **104**, 223601 (2010).
116. S. E. Harris, "Nonlocal modulation of entangled photons," Phys. Rev. A **78**, 021807 (2008).
117. C. Belthangady, S. Du, C.-S. Chuu, *et al.*, "Modulation and measurement of time-energy entangled photons," Phys. Rev. A **80**, 031803 (2009).
118. S. Sensarn, G. Y. Yin, and S. E. Harris, "Observation of nonlocal modulation with entangled photons," Phys. Rev. Lett. **103**, 163601 (2009).
119. L. Olislager, J. Cussey, A. T. Nguyen, *et al.*, "Frequency-bin entangled photons," Phys. Rev. A **82**, 013804 (2010).
120. J. M. Lukens, O. D. Odele, D. E. Leaird, *et al.*, "Electro-optic modulation for high-speed characterization of entangled photon pairs," Opt. Lett. **40**, 5331–5334 (2015).
121. M. Karpinski, M. Jachura, L. J. Wright, *et al.*, "Bandwidth manipulation of quantum light by an electro-optic time lens," Nat. Photonics **11**, 53–57 (2017).
122. C. Joshi, B. M. Sparkes, A. Farsi, *et al.*, "Picosecond-resolution single-photon time lens for temporal mode quantum processing," Optica **9**, 364–373 (2022).
123. L. J. Wright, M. Karpiński, C. Söller, *et al.*, "Spectral shearing of quantum light pulses by electro-optic phase modulation," Phys. Rev. Lett. **118**, 023601 (2017).
124. J. Capmany and C. R. Fernández-Pousa, "Quantum model for electro-optical phase modulation," J. Opt. Soc. Am. B **27**, A119–A129 (2010).
125. J. Capmany and C. Fernández-Pousa, "Quantum modelling of electro-optic modulators," Laser Photon. Rev. **5**, 750–772 (2011).
126. P. Imany, O. D. Odele, M. S. Alshaykh, *et al.*, "Frequency-domain Hong–Ou–Mandel interference with linear optics," Opt. Lett. **43**, 2760–2763 (2018).
127. H.-P. Lo and H. Takesue, "Precise tuning of single-photon frequency using an optical single sideband modulator," Optica **4**, 919–923 (2017).
128. F.-Y. Wang, B.-S. Shi, and G.-C. Guo, "Observation of time correlation function of multimode two-photon pairs on a rubidium D_2 line," Opt. Lett. **33**, 2191–2193 (2008).
129. X. Guo, Y. Mei, and S. Du, "Testing the Bell inequality on frequency-bin entangled photon pairs using time-resolved detection," Optica **4**, 388–392 (2017).
130. R. Ikuta, R. Tani, M. Ishizaki, *et al.*, "Frequency-multiplexed photon pairs over 1000 modes from a quadratic nonlinear optical waveguide resonator with a singly resonant configuration," Phys. Rev. Lett. **123**, 193603 (2019).
131. H.-H. Lu, N. B. Lingaraju, D. E. Leaird, *et al.*, "High-dimensional discrete Fourier transform gates with a quantum frequency processor," Opt. Express **30**, 10126–10134 (2022).
132. S. Seshadri, H.-H. Lu, D. E. Leaird, *et al.*, "Complete frequency-bin Bell basis synthesizer," Phys. Rev. Lett. **129**, 230505 (2022).
133. M. Avenhaus, A. Eckstein, P. J. Mosley, *et al.*, "Fiber-assisted single-photon spectrograph," Opt. Lett. **34**, 2873–2875 (2009).
134. A. O. C. Davis, P. M. Saulnier, M. Karpiński, *et al.*, "Pulsed single-photon spectrometer by frequency-to-time mapping using chirped fiber Bragg gratings," Opt. Express **25**, 12804–12811 (2017).
135. C. K. Hong, Z. Y. Ou, and L. Mandel, "Measurement of subpicosecond time intervals between two photons by interference," Phys. Rev. Lett. **59**, 2044–2046 (1987).
136. A. Eckstein and C. Silberhorn, "Broadband frequency mode entanglement in waveguided parametric downconversion," Opt. Lett. **33**, 1825–1827 (2008).
137. A. Fedrizzi, T. Herbst, M. Aspelmeyer, *et al.*, "Anti-symmetrization reveals hidden entanglement," New J. Phys. **11**, 103052 (2009).
138. S. Ramelow, L. Ratschbacher, A. Fedrizzi, *et al.*, "Discrete tunable color entanglement," Phys. Rev. Lett. **103**, 253601 (2009).
139. F. Kaneda, H. Suzuki, R. Shimizu, *et al.*, "Direct generation of frequency-bin entangled photons via two-period quasi-phase-matched parametric downconversion," Opt. Express **27**, 1416–1424 (2019).
140. S. Merkouche, V. Thiel, A. O. C. Davis, *et al.*, "Heralding multiple photonic pulsed Bell pairs via frequency-resolved entanglement swapping," Phys. Rev. Lett. **128**, 063602 (2022).
141. C. Chen, C. Xu, A. Riazi, *et al.*, "Telecom-band hyperentangled photon pairs from a fiber-based source," Phys. Rev. A **105**, 043702 (2022).
142. N. B. Lingaraju, H.-H. Lu, S. Seshadri, *et al.*, "Quantum frequency combs and Hong–Ou–Mandel interferometry: the role of spectral phase coherence," Opt. Express **27**, 38683–38697 (2019).
143. D. Rieländer, A. Lenhard, O. J. Farìas, *et al.*, "Frequency-bin entanglement of ultra-narrow band non-degenerate photon pairs," Quantum Sci. Technol. **3**, 014007 (2018).
144. P. Imany, J. A. Jaramillo-Villegas, M. S. Alshaykh, *et al.*, "High-dimensional optical quantum logic in large operational spaces," npj Quantum Inf. **5**, 59 (2019).
145. R. Fujimoto, T. Yamazaki, T. Kobayashi, *et al.*, "Entanglement distribution using a biphoton frequency comb compatible with DWDM technology," Opt. Express **30**, 36711–36716 (2022).
146. K.-C. Chang, X. Cheng, M. C. Sarihan, *et al.*, "648 Hilbert-space dimensionality in a biphoton frequency comb: entanglement of formation and Schmidt mode decomposition," npj Quantum Inf. **7**, 48 (2021).
147. H. Mahmudlu, R. Johanning, A. van Rees, *et al.*, "Fully on-chip photonic turnkey quantum source for entangled qubit/qudit state generation," Nat. Photonics **17**, 518–524 (2023).
148. F. A. Sabattoli, L. Gianini, A. Simbula, *et al.*, "Silicon source of frequency-bin entangled photons," Opt. Lett. **47**, 6201–6204 (2022).
149. M. Liscidini and J. E. Sipe, "Scalable and efficient source of entangled frequency bins," Opt. Lett. **44**, 2625–2628 (2019).
150. S. Francesconi, F. Baboux, A. Raymond, *et al.*, "Engineering two-photon wavefunction and exchange statistics in a semiconductor chip," Optica **7**, 316–322 (2020).
151. W. Wen, Z. Chen, L. Lu, *et al.*, "Realizing an entanglement-based multiuser quantum network with integrated photonics," Phys. Rev. Appl. **18**, 024059 (2022).
152. M. Raymer, S. van Enk, C. McKinstrie, *et al.*, "Interference of two photons of different color," Opt. Commun. **283**, 747–752 (2010).
153. T. Kobayashi, R. Ikuta, S. Yasui, *et al.*, "Frequency-domain Hong–Ou–Mandel interference," Nat. Photonics **10**, 441–444 (2016).
154. T. Kobayashi, D. Yamazaki, K. Matsuki, *et al.*, "Mach-Zehnder interferometer using frequency-domain beamsplitter," Opt. Express **25**, 12052–12060 (2017).
155. H.-H. Lu, E. M. Simmerman, P. Lougovski, *et al.*, "Fully arbitrary control of frequency-bin qubits," Phys. Rev. Lett. **125**, 120503 (2020).
156. P. Imany, N. B. Lingaraju, M. S. Alshaykh, *et al.*, "Probing quantum walks through coherent control of high-dimensionally entangled photons," Sci. Adv. **6**, eaba8066 (2020).
157. E. Knill, R. Laflamme, and G. J. Milburn, "A scheme for efficient quantum computation with linear optics," Nature **409**, 46–52 (2001).
158. H.-H. Lu, N. Klco, J. M. Lukens, *et al.*, "Simulations of subatomic many-body physics on a quantum frequency processor," Phys. Rev. A **100**, 012320 (2019).
159. N. J. Cerf, M. Bourennane, A. Karlsson, *et al.*, "Security of quantum key distribution using -level systems," Phys. Rev. Lett. **88**, 127902 (2002).
160. S. Ecker, F. Bouchard, L. Bulla, *et al.*, "Overcoming noise in entanglement distribution," Phys. Rev. X **9**, 041042 (2019).
161. T. Vértesi, S. Pironio, and N. Brunner, "Closing the detection loophole in Bell experiments using qudits," Phys. Rev. Lett. **104**, 060401 (2010).
162. C. Reimer, S. Sciara, P. Roztocki, *et al.*, "High-dimensional one-way quantum processing implemented on -level cluster states," Nat. Phys. **15**, 148–153 (2019).
163. Keysight, "M8100 series arbitrary waveform generators," 2023, https://www.keysight.com.
164. W. K. Wootters and B. D. Fields, "Optimal state-determination by mutually unbiased measurements," Ann. Phys. **191**, 363–381 (1989).
165. T. Durt, B.-G. Englert, I. Bengtsson, *et al.*, "On mutually unbiased bases," Int. J. Quantum Inf. **8**, 535–640 (2010).
166. U. A. Javid, R. Lopez-Rios, J. Ling, *et al.*, "Chip-scale simulations in a quantum-correlated synthetic space," Nat. Photonics **17**, 883–890 (2023).
167. M. Cabrejo-Ponce, A. L. M. Muniz, M. Huber, *et al.*, "High-dimensional entanglement for quantum communication in the frequency domain," Laser Photon. Rev. **17**, 2201010 (2023).
168. P. Imany, O. D. Odele, J. A. Jaramillo-Villegas, *et al.*, "Characterization of coherent quantum frequency combs using electro-optic phase modulation," Phys. Rev. A **97**, 013813 (2018).
169. S. Seshadri, N. Lingaraju, H.-H. Lu, *et al.*, "Nonlocal subpicosecond delay metrology using spectral quantum interference," Optica **9**, 1339–1346 (2022).
170. A. W. Elshaari, W. Pernice, K. Srinivasan, *et al.*, "Hybrid integrated quantum photonic circuits," Nat. Photonics **14**, 285–298 (2020).

171. M. S. Dahlem, C. W. Holzwarth, A. Khilo, *et al.*, "Reconfigurable multi-channel second-order silicon microring-resonator filterbanks for on-chip WDM systems," Opt. Express **19**, 306–316 (2011).
172. B. E. Nussbaum, A. J. Pizzimenti, N. B. Lingaraju, *et al.*, "Design methodologies for integrated quantum frequency processors," J. Lightwave Technol. **40**, 7648–7657 (2022).
173. X. Jiang, D. Pak, A. Nandi, *et al.*, "Rare earth-implanted lithium niobate: properties and on-chip integration," Appl. Phys. Lett. **115**, 071104 (2019).
174. Y. Hu, M. Yu, D. Zhu, *et al.*, "On-chip electro-optic frequency shifters and beam splitters," Nature **599**, 587–593 (2021).
175. M. D. Eisaman, J. Fan, A. Migdall, *et al.*, "Invited review article: single-photon sources and detectors," Rev. Sci. Instrum. **82**, 071101 (2011).
176. I. Aharonovich, D. Englund, and M. Toth, "Solid-state single-photon emitters," Nat. Photonics **10**, 631–641 (2016).
177. C. Couteau, S. Barz, T. Durt, *et al.*, "Applications of single photons to quantum communication and computing," Nat. Rev. Phys. **5**, 326–338 (2023).
178. B. E. Little, S. T. Chu, H. A. Haus, *et al.*, "Microring resonator channel dropping filters," J. Lightwave Technol. **15**, 998–1005 (1997).
179. W. Bogaerts, P. De Heyn, T. Van Vaerenbergh, *et al.*, "Silicon microring resonators," Laser Photon. Rev. **6**, 47–73 (2012).
180. J. Hryniewicz, P. Absil, B. Little, *et al.*, "Higher order filter response in coupled microring resonators," IEEE Photon. Technol. Lett. **12**, 320–322 (2000).
181. B. E. Little, S. T. Chu, P. P. Absil, *et al.*, "Very high-order microring resonator filters for WDM applications," IEEE Photon. Technol. Lett. **16**, 2263–2265 (2004).
182. N. Sinclair, E. Saglamyurek, H. Mallahzadeh, *et al.*, "Spectral multiplexing for scalable quantum photonics using an atomic frequency comb quantum memory and feed-forward control," Phys. Rev. Lett. **113**, 053603 (2014).
183. E. Saglamyurek, N. Sinclair, J. A. Slater, *et al.*, "An integrated processor for photonic quantum states using a broadband light–matter interface," New J. Phys. **16**, 065019 (2014).
184. A. Seri, D. Lago-Rivera, A. Lenhard, *et al.*, "Quantum storage of frequency-multiplexed heralded single photons," Phys. Rev. Lett. **123**, 080502 (2019).
185. M. Hosseini, B. M. Sparkes, G. Hétet, *et al.*, "Coherent optical pulse sequencer for quantum applications," Nature **461**, 241–245 (2009).
186. M. Hosseini, B. M. Sparkes, G. Campbell, *et al.*, "High efficiency coherent optical memory with warm rubidium vapour," Nat. Commun. **2**, 174 (2011).
187. M. Hosseini, G. Campbell, B. M. Sparkes, *et al.*, "Unconditional room-temperature quantum memory," Nat. Phys. **7**, 794–798 (2011).
188. M. L. Chan, Z. Aqua, A. Tiranov, *et al.*, "Quantum state transfer between a frequency-encoded photonic qubit and a quantum-dot spin in a nanophotonic waveguide," Phys. Rev. A **105**, 062445 (2022).
189. T. Zhong, J. M. Kindem, J. Rochman, *et al.*, "Interfacing broadband photonic qubits to on-chip cavity-protected rare-earth ensembles," Nat. Commun. **8**, 14107 (2017).
190. T. Zhong, J. M. Kindem, J. G. Bartholomew, *et al.*, "Nanophotonic rare-earth quantum memory with optically controlled retrieval," Science **357**, 1392–1395 (2017).
191. J. Lavoie, J. M. Donohue, L. G. Wright, *et al.*, "Spectral compression of single photons," Nat. Photonics **7**, 363–366 (2013).
192. K. V. Myilswamy and A. M. Weiner, "Spectral compression using time-varying cavities," Opt. Lett. **45**, 5688–5691 (2020).
193. K. V. Myilswamy and A. M. Weiner, "Temporal modulation of a spectral compressor for efficient quantum storage," Opt. Lett. **47**, 1387–1390 (2022).
194. F. Sośnicki, M. Mikołajczyk, A. Golestani, *et al.*, "Interface between picosecond and nanosecond quantum light pulses," Nat. Photonics **17**, 761–766 (2023).
195. EOSpace, "Phase modulators," 2023, https://www.eospace.com/phase-modulator.
196. ixBlue, "MPZ-LN-40-00-P-P-FA-FA," 2023, https://www.ixblue.com/north-america/store/mpz-ln-40-00-p-p-fa-fa/.
197. I-VI, "Waveshaper 1000A programmable optical filter," 2023, https://ii-vi.com/product/waveshaper-1000a-programmable-optical-filter/.
198. G. Moody, V. J. Sorger, D. J. Blumenthal, *et al.*, "2022 roadmap on integrated quantum photonics," J. Phys. Photon. **4**, 012501 (2022).
199. R. Soref and B. Bennett, "Electrooptical effects in silicon," IEEE J. Quant. Electron. **23**, 123–129 (1987).
200. G. T. Reed, G. Mashanovich, F. Y. Gardes, *et al.*, "Silicon optical modulators," Nat. Photonics **4**, 518–526 (2010).
201. L. Chrostowski and M. Hochberg, *Silicon Photonics Design: From Devices to Systems* (Cambridge University, 2015).
202. C. Wang, M. Zhang, X. Chen, *et al.*, "Integrated lithium niobate electro-optic modulators operating at CMOS-compatible voltages," Nature **562**, 101–104 (2018).
203. T. Ren, M. Zhang, C. Wang, *et al.*, "An integrated low-voltage broadband lithium niobate phase modulator," IEEE Photon. Technol. Lett. **31**, 889–892 (2019).
204. L. Alloatti, R. Palmer, S. Diebold, *et al.*, "100 GHz silicon–organic hybrid modulator," Light Sci. Appl. **3**, e173 (2014).
205. C. Kieninger, Y. Kutuvantavida, D. L. Elder, *et al.*, "Ultra-high electro-optic activity demonstrated in a silicon-organic hybrid modulator," Optica **5**, 739–748 (2018).
206. S. Ummethala, J. N. Kemal, A. S. Alam, *et al.*, "Hybrid electro-optic modulator combining silicon photonic slot waveguides with high-k radio-frequency slotlines," Optica **8**, 511–519 (2021).
207. P. Bhasker, J. Norman, J. Bowers, *et al.*, "Intensity and phase modulators at 1.55 μm in GaAs/AlGaAs layers directly grown on silicon," J. Lightwave Technol. **36**, 4205–4210 (2018).
208. P. Bhasker, J. Norman, J. Bowers, *et al.*, "Low voltage, high optical power handling capable, bulk compound semiconductor electro-optic modulators at 1550 nm," J. Lightwave Technol. **38**, 2308–2314 (2020).
209. S. Dogru and N. Dagli, "0.77-V drive voltage electro-optic modulator with bandwidth exceeding 67 GHz," Opt. Lett. **39**, 6074–6077 (2014).
210. Y. Ogiso, J. Ozaki, Y. Ueda, *et al.*, "80-GHz bandwidth and 1.5-V Vπ InP-based IQ modulator," J. Lightwave Technol. **38**, 249–255 (2019).
211. A. Agarwal, P. Toliver, R. Menendez, *et al.*, "Fully programmable ring-resonator-based integrated photonic circuit for phase coherent applications," J. Lightwave Technol. **24**, 77–87 (2006).
212. M. H. Khan, H. Shen, Y. Xuan, *et al.*, "Ultrabroad-bandwidth arbitrary radiofrequency waveform generation with a silicon photonic chip-based spectral shaper," Nat. Photonics **4**, 117–122 (2010).
213. J. Wang, H. Shen, L. Fan, *et al.*, "Reconfigurable radio-frequency arbitrary waveforms synthesized in a silicon photonic chip," Nat. Commun. **6**, 5957 (2015).
214. M. Bahadori, M. Nikdast, Q. Cheng, *et al.*, "Universal design of waveguide bends in silicon-on-insulator photonics platform," J. Lightwave Technol. **37**, 3044–3054 (2019).
215. X. Ji, J. Liu, J. He, *et al.*, "Compact, spatial-mode-interaction-free, ultralow-loss, nonlinear photonic integrated circuits," Commun. Phys. **5**, 84 (2022).
216. D. Onural, H. Gevorgyan, B. Zhang, *et al.*, "Ultra-high Q resonators and sub-GHz bandwidth second order filters in an SOI foundry platform," in *Optical Fiber Communication Conference* (Optica, 2020), pp. W1A.4.
217. L. M. Cohen, S. Fatema, V. V. Wankhade, *et al.*, "Fine-resolution silicon photonic wavelength-selective switch using hybrid multimode racetrack resonators," arXiv, arXiv:2309.17222v1 (2023).
218. M. Zhang, C. Wang, Y. Hu, *et al.*, "Electronically programmable photonic molecule," Nat. Photonics **13**, 36–40 (2019).
219. H. Gevorgyan, A. Khilo, and M. A. Popović, "Active-cavity photonic molecule optical data wavelength converter for silicon photonics platforms," arXiv, arXiv:2005.04989 (2020).
220. S. Buddhiraju, A. Dutt, M. Minkov, *et al.*, "Arbitrary linear transformations for photons in the frequency synthetic dimension," Nat. Commun. **12**, 2401 (2021).
221. S. M. Foreman, K. W. Holman, D. D. Hudson, *et al.*, "Remote transfer of ultrastable frequency references via fiber networks," Rev. Sci. Instrum. **78**, 021101 (2007).
222. Ł. Śliwczyński, P. Krehlik, and M. Lipiński, "Optical fibers in time and frequency transfer," Meas. Sci. Technol. **21**, 075302 (2010).
223. M. Xin, K. Şafak, M. Y. Peng, *et al.*, "Attosecond precision multi-kilometer laser-microwave network," Light Sci. Appl. **6**, e16187 (2017).
224. M. Lipiński, T. Włostowski, J. Serrano, *et al.*, "White rabbit: a PTP application for robust sub-nanosecond synchronization," in *IEEE International Symposium on Precision Clock Synchronization for Measurement, Control, and Communication* (2011), pp. 25–30.
225. M. Rizzi, M. Lipinski, P. Ferrari, *et al.*, "White Rabbit clock synchronization: ultimate limits on close-in phase noise and short-term stability due to FPGA implementation," IEEE Trans. Ultrason. Ferroelectr. Freq. Control. **65**, 1726–1737 (2018).

226. M. Alshowkan, P. G. Evans, B. P. Williams, *et al.*, "Advanced architectures for high-performance quantum networking," J. Opt. Commun. Netw. **14**, 493–499 (2022).
227. I. A. Burenkov, A. Semionov, Hala, *et al.*, "Synchronization and coexistence in quantum networks," Opt. Express **31**, 11431–11446 (2023).
228. V. J. Urick, F. Bucholtz, J. D. McKinney, *et al.*, "Long-haul analog photonics," J. Lightwave Technol. **29**, 1182–1205 (2011).
229. W. Pfaff, B. J. Hensen, H. Bernien, *et al.*, "Unconditional quantum teleportation between distant solid-state quantum bits," Science **345**, 532–535 (2014).
230. S. L. N. Hermans, M. Pompili, H. K. C. Beukers, *et al.*, "Qubit teleportation between non-neighbouring nodes in a quantum network," Nature **605**, 663–668 (2022).
231. L.-M. Duan and H. J. Kimble, "Efficient engineering of multiatom entanglement through single-photon detections," Phys. Rev. Lett. **90**, 253601 (2003).
232. N. Sangouard, C. Simon, H. De Riedmatten, *et al.*, "Quantum repeaters based on atomic ensembles and linear optics," Rev. Mod. Phys. **83**, 33–80 (2011).
233. C. Monroe, R. Raussendorf, A. Ruthven, *et al.*, "Large-scale modular quantum-computer architecture with atomic memory and photonic interconnects," Phys. Rev. A **89**, 022317 (2014).
234. L.-M. Duan, M. D. Lukin, J. I. Cirac, *et al.*, "Long-distance quantum communication with atomic ensembles and linear optics," Nature **414**, 413–418 (2001).
235. X.-L. Feng, Z.-M. Zhang, X.-D. Li, *et al.*, "Entangling distant atoms by interference of polarized photons," Phys. Rev. Lett. **90**, 217902 (2003).
236. C. Simon and W. T. M. Irvine, "Robust long-distance entanglement and a loophole-free Bell test with ions and photons," Phys. Rev. Lett. **91**, 110405 (2003).
237. S.-Y. Lan, S. D. Jenkins, T. Chanelière, *et al.*, "Dual-species matter qubit entangled with light," Phys. Rev. Lett. **98**, 123602 (2007).
238. W. Dür, G. Vidal, and J. I. Cirac, "Three qubits can be entangled in two inequivalent ways," Phys. Rev. A **62**, 062314 (2000).
239. P. Lougovski, S. J. van Enk, K. S. Choi, *et al.*, "Verifying multipartite mode entanglement of W states," New J. Phys. **11**, 063029 (2009).
240. K. S. Choi, A. Goban, S. B. Papp, *et al.*, "Entanglement of spin waves among four quantum memories," Nature **468**, 412–416 (2010).
241. M. Żukowski, A. Zeilinger, M. A. Horne, *et al.*, "'Event-ready-detectors' Bell experiment via entanglement swapping," Phys. Rev. Lett. **71**, 4287–4290 (1993).
242. J.-W. Pan, D. Bouwmeester, H. Weinfurter, *et al.*, "Experimental entanglement swapping: entangling photons that never interacted," Phys. Rev. Lett. **80**, 3891–3894 (1998).
243. G. Vittorini, D. Hucul, I. V. Inlek, *et al.*, "Entanglement of distinguishable quantum memories," Phys. Rev. A **90**, 040302 (2014).
244. T.-M. Zhao, H. Zhang, J. Yang, *et al.*, "Entangling different-color photons via time-resolved measurement and active feed forward," Phys. Rev. Lett. **112**, 103602 (2014).
245. D. L. Moehring, M. J. Madsen, K. C. Younge, *et al.*, "Quantum networking with photons and trapped atoms (invited)," J. Opt. Soc. Am. B **24**, 300–315 (2007).
246. J.-M. Mérolla, Y. Mazurenko, J.-P. Goedgebuer, *et al.*, "Quantum cryptographic device using single-photon phase modulation," Phys. Rev. A **60**, 1899–1905 (1999).
247. J.-M. Mérolla, Y. Mazurenko, J.-P. Goedgebuer, *et al.*, "Single-photon interference in sidebands of phase-modulated light for quantum cryptography," Phys. Rev. Lett. **82**, 1656–1659 (1999).
248. M. Bloch, S. W. McLaughlin, J.-M. Merolla, *et al.*, "Frequency-coded quantum key distribution," Opt. Lett. **32**, 301–303 (2007).
249. R. Xue, X. Liu, H. Li, *et al.*, "Measurement-device-independent quantum key distribution of frequency-nondegenerate photons," Phys. Rev. Appl. **17**, 024045 (2022).
250. I. Herbauts, B. Blauensteiner, A. Poppe, *et al.*, "Demonstration of active routing of entanglement in a multi-user network," Opt. Express **21**, 29013–29024 (2013).
251. S. Wengerowsky, S. K. Joshi, F. Steinlechner, *et al.*, "An entanglement-based wavelength-multiplexed quantum communication network," Nature **564**, 225–228 (2018).
252. F. Laudenbach, B. Schrenk, M. Achleitner, *et al.*, "Flexible cloud/user-centric entanglement and photon pair distribution with synthesizable optical router," IEEE J. Sel. Top. Quantum Electron. **26**, 6400509 (2020).
253. S. K. Joshi, D. Aktas, S. Wengerowsky, *et al.*, "A trusted node–free eight-user metropolitan quantum communication network," Sci. Adv. **6**, eaba0959 (2020).
254. N. B. Lingaraju, H.-H. Lu, S. Seshadri, *et al.*, "Adaptive bandwidth management for entanglement distribution in quantum networks," Optica **8**, 329–332 (2021).
255. F. Appas, F. Baboux, M. I. Amanti, *et al.*, "Flexible entanglement-distribution network with an AlGaAs chip for secure communications," npj Quantum Inf. **7**, 118 (2021).
256. M. Alshowkan, B. P. Williams, P. G. Evans, *et al.*, "Reconfigurable quantum local area network over deployed fiber," PRX Quantum **2**, 040304 (2021).